THE UNIVERSITY OF MICHIGAN

INDUSTRY PROGRAM OF THE COLLEGE OF ENGINEERING

THE KINETICS OF CUMENE HYDROPEROXIDE DECOMPOSITION AS CATALYZED BY ACID ION EXCHANGE RESIN

James E. Marberry

A dissertation submitted in partial fulfillment
of the requirements for the degree of
Doctor of Philosophy in The
University of Michigan
1960

February, 1960

IP-416

ACKNOWLEDGMENTS

The author wishes to express his appreciation to the members of the committee, Professors S. W. Churchill, K. F. Gordon, D. W. McCready, and R. W. Parry, for their discussion and comments on the ideas considered in this work, and particularly to Professor J. T. Banchero, for his guidance during the experimental work; to Dow Chemical Company and Hercules Powder Company, who supplied the catalyst and reactant; and to Phillips Petroleum Company and Monsanto Chemical Company, whose financial assistance made the work possible.

TABLE OF CONTENTS

	Page
ACKNOWLEDGEMENTS	ii
LIST OF TABLES	v
LIST OF FIGURES	vi
NOMENCLATURE	vii
INTRODUCTION	1
THEORY	3
The Decomposition Reaction	3
The Nature of the Catalyst	10
Derivation of the Mathematical Model	17
EQUIPMENT	30
MATERIALS	36
EXPERIMENTAL PROCEDURE	39
Analytical Methods	41
EXPERIMENTAL RESULTS	46
Effect of Flow Rate	47
Precision and Reproducibility of k Value Measurements	49
Effect of Water Concentration	51
Effect of Particle Size and Resin Grade	54
Effect of Temperature	55
Effect of CHP Concentration	56
The Yield of Phenol	60
DISCUSSION	62
Phase Distribution	62
Behavior of the Catalyst	64
Comparison with the Homogeneous Rate	67
The Use of Cumene as Solvent	69
CORRELATION	72

TABLE OF CONTENTS (CONT'D)

	Page
CONCLUSIONS	90
APPENDIX A Tabulation of Experimental Data	92
APPENDIX B Estimation of Particle Temperature	97
APPENDIX C Sample Calculations and Experimental Measurements	101
BIBLIOGRAPHY	105

LIST OF TABLES

Table		Page
I	Effect of Flow Rate on the k Value at a High Reaction Rate	48
II	Effect of Flow Rate on the k Value at a Low Reaction Rate	49
III	Reproducibility of k Values	51
IV	Effect of Particle Size on k Value	55
V	Values of k for Correlation	73

LIST OF FIGURES

Figure		Page
1	Representation of Catalyst Gel Structure.....	12
2	Spherical Element in Catalyst Particle.....	19
3	Differential Element of Catalyst in Reactor.....	27
4	Diagrammatic Sketch of Equipment.....	31
5	Cutaway View of Reactor Unit.....	32
6	Effect of Water Content on k; 32-35 mesh Dowex 50 X 8, 10% CHP.....	52
7	Effect of Water Content on k; 60-65 mesh Dowex 50 X 8, 10% CHP.....	53
8	Effect of Temperature on k; 60-65 mesh Dowex 50 X 8....	57
9	Effect of Temperature on k; 115-150 mesh Dowex 50 X 8..	58
10	Effect of CHP Concentration on k; 32-35 mesh Dowex 50 X 8, 50°C.....	59
11	Effect of Water on k Using Cumene as Solvent.....	70
12	ϕ Ratio versus α.....	74
13	Effect of Temperature on α.....	76
14	Effect of Water Concentration on α.....	77
15	Correlation of Temperature.....	80
16	Correlation of the Effect of Water Concentration on λ..	82
17	Correlation of the Effect of CHP Concentration on λ....	84
18	Comparison of Correlation with Experimental Data; C_w = 0.00074 moles water/cc.....	87
19	Comparison of Correlation with Experimental Data; C_w = 0.00161 moles water/cc.....	88
20	Comparison of Correlation with Experimental Data; C_w = 0.00267 moles water/cc.....	89

NOMENCLATURE

a_1 a_2	constants
A, A'	constants
A	area, cm.^{2}
b	thermal conductivity, cal per (cm.)(min.)(°C)
c_1 c_2	constants
CHP	cumene hydroperoxide
C_j	concentration of component j in the liquid phase, mol./cc.
C'	concentration of CHP in the resin phase, mol. CHP/cc.
D	diffusivity of CHP in the resin phase, cm.^{2}/min.
E	activation energy, cal./mol.
g	mg. phenol/50 ml. soln.
ΔH	heat of reaction, cal absorbed/mol. CHP decomposed
H_j	enthalpy of component j, cal./mol.
j	any component
k	experimental variable, gm. per (min.)(equiv. H^+), defined, Equation 33.
k_1	rate constant, min.$^{-1}$, except sec.$^{-1}$, p. 7.
k_2	rate constant, cm.^{3} per (mol. H_3O^+)(min.) and kg. per (mol. H_3O^+)(sec.)
K	chemical equilibrium constant
(L)	large size resin (32-35 mesh)
(M)	medium size resin (60-65 mesh)
m	acid concentration, equiv. H^+/cc. catalyst
dn	differential quantity of equivalents in catalyst bed.
N	total equivalents in reactor

NOMENCLATURE (CONT'D)

n, n'	order of reaction
q	heat diffusion rate, cal. per (min.)(cm.^{2})
Q_j	heat of combustion, kg. cal./mol. j
r	particle radius, cm.
R	reaction rate, mol. CHP decomposed per (min.)(cc.); gas constant, cal. per (mol.)(°C)
S	entropy, cal. per (mol.)(°C)
(S)	small size resin (115-150 mesh)
T	temperature, °C and °K
v	sample volume, cc.
v'	aliquot volume, cc.
V	volume (general) volume of titrating reagent, cc.
W	feed flow rate, gm./min.
w	CHP diffusion rate, mol. CHP per (min.)(cm.^{2})
x	radius within particle, cm.
α	constant, cm.$^{-1}$ $\alpha = (k_1/D)^{\frac{1}{2}}$
λ	phase distribution coefficient for CHP, defined, Equation 29
ρ	feed density, gm/cc.
θ	time
ϕ	resin efficiency factor, dimensionless, defined, Equation 25

Subscripts

a	acetone
c	cumene hydroperoxide

f	outlet or final state
i	inlet or initial state
j	any component
p	phenol
s	particle surface
w	water

INTRODUCTION

The commercial production of phenol is accomplished by several competitive processes. One of these processes consists of the alkylation of benzene to cumene (isopropyl benzene), oxidation of the cumene to cumene hydroperoxide, and decomposition of the cumene hydroperoxide with a catalyst (10% sulfuric acid) to phenol and acetone. The final reaction of this sequence takes place in a two phase mixture (aqueous-organic). Separation of the phenol and recovery of the acid from this mixture are steps which contribute significantly to the cost of phenol production by this method.

Ion exchange resins in acid form have been used successfully as catalysts in laboratory studies of reactions such as hydrolysis and esterification which are catalyzed by mineral acids. The use of an acid resin as the catalyst for the decomposition reaction of the commercial phenol process was therefore indicated as a suitable subject for study. Lower production costs may result from the use of a solid acid which can be separated easily from the reaction mixture.

The primary reaction taking place when cumene hydroperoxide (CHP) is decomposed by strong acid is

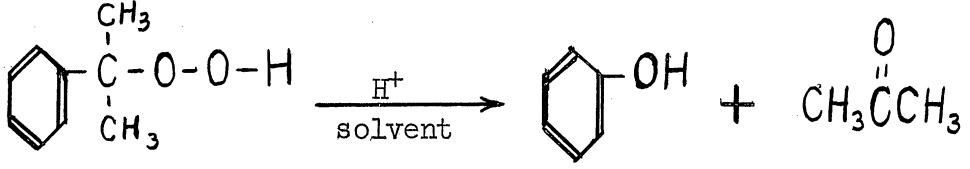

(1)

CHP phenol acetone

The reaction is sufficiently exothermic that this property must be considered in experimentation and correlation.

Cumene hydroperoxide can decompose to a number of products. Strong acids give phenol and the associated product acetone in 90% yield, while other catalysts and the thermal reaction give low phenol yields. The use of an ion exchange resin which is a strong acid is thus indicated as necessary in a study oriented toward the commercial process.

The catalyst used in this investigation was Dowex 50 in acid form, a sulfonated, cross-linked, polystyrene resin available in a number of particle size ranges, degrees of cross-linking, and color grades. The sulfonic acid groups in this resin have the required strong acid property. The use of an ion exchange resin as a successful catalyst requires that the reactant and products can diffuse freely through the resin to and away from the acid groups which exist uniformly throughout the resin and also that the reaction environment does not destroy the resin's catalytic activity. The resin absorbs liquids within its gel structure, and the reaction takes place in this internal liquid phase.

The aim of this study was to determine if Dowex 50 is a suitable catalyst for the decomposition of cumene hydroperoxide to phenol and to measure the rate of decomposition using acid Dowex 50 particles in a tubular flow reactor under steady state conditions. The nate was desired as a function of the parameters temperature, flow rate, feed composition, and catalyst type (particle size and degree of cross-linking). A rate expression applicable to the data was derived, and supplementary work included measurement of the yield of phenol and observation of the stability of the catalyst.

THEORY

The Decomposition Reaction

Organic peroxides can be induced to decompose by several activating agents, heat, acids, and bases being common ones. Two mechanisms of decomposition are postulated, one proceeding through free radicals, the other through an ionic intermediate.

The route through which a given reactant will decompose is determined by the activating agent, polarity of the medium, and the symmetry and nature of the reactant structure. Symmetrical peroxides have been found to decompose preferentially to free radicals, and the preference for the free radical mechanism is lessened as the asymmetry of the molecule increases.[1] An example of a symmetrical peroxide is benzoyl peroxide (I), which decomposes to two identical free radicals, almost regardless of solvent changes or acid catalysis:

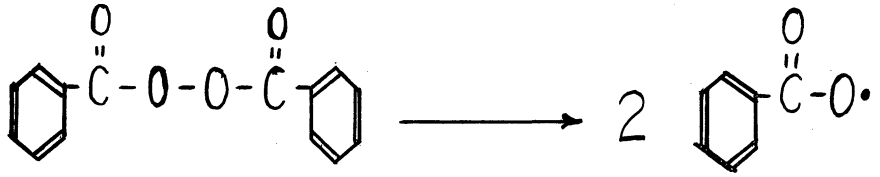

(I) (2)

The effect of environment change is illustrated by the decomposition of p-methoxy-p'-nitrobenzoyl peroxide (II). It decomposes to equal quantities of p-nitrobenzoic acid (III) and anisic acid (IV) in benzene but gives reduced amounts of anisic acid in acid or polar solvents.[2] The rearrangement of an ionic intermediate is suggested to

account for the loss of anisic acid; the initial step in benzene is assumed to be the separation into two free radicals, while in polar solvents or with acid catalysts the suggested first step is separation into two ions:

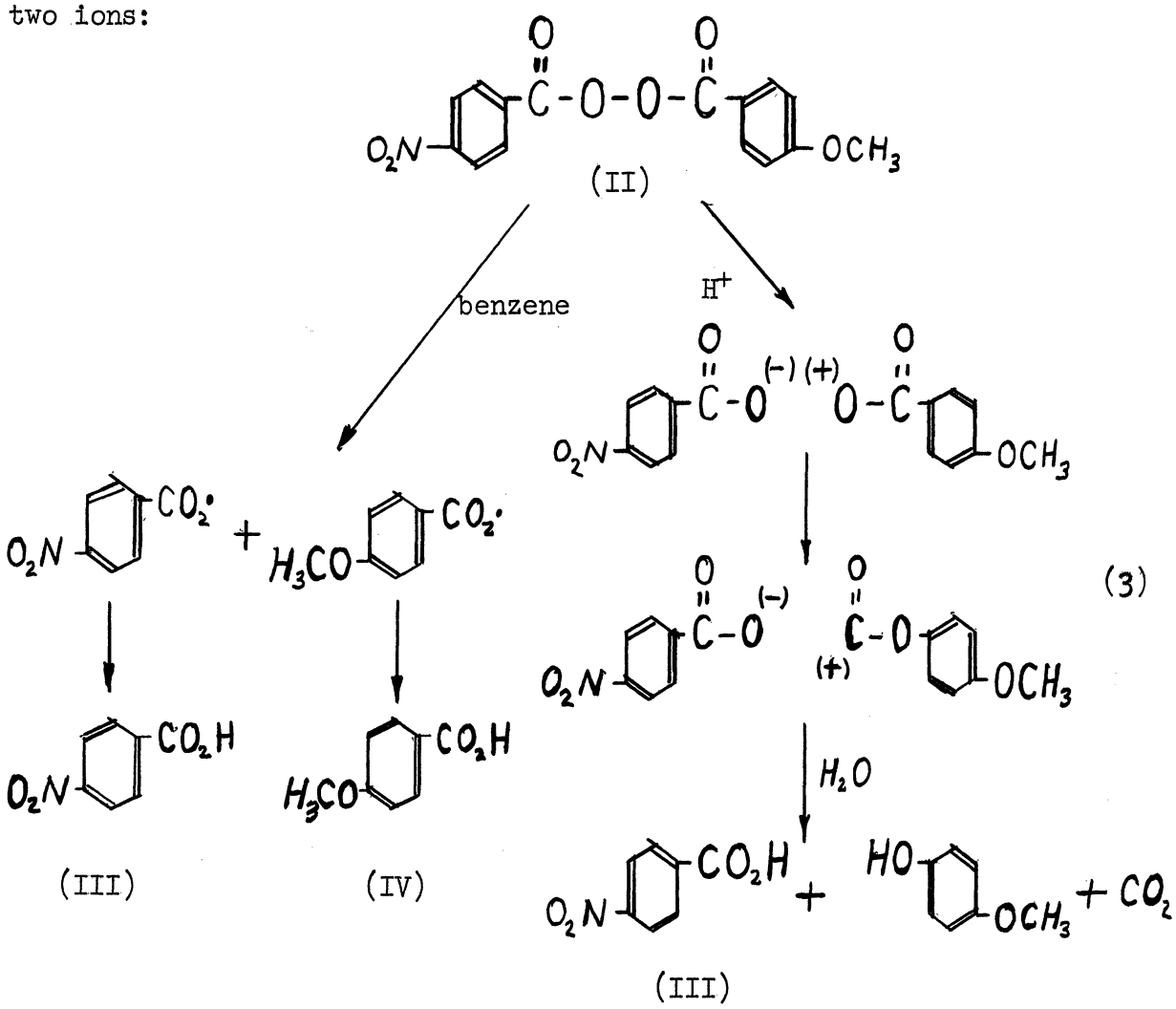

The mechanism of decomposition of a given reactant can be studied by its effect on polymerizable material and by isolation of the reaction products. The chain-initiating potential of the free radicals produced by the symmetrical cleavage of a peroxide has been well studied, as has the ease of migration of a positive charge to a more stable position on a carbon structure. The effect of conditions such as high acidity

or polarity is to increase the stability of an ionic separation, allowing the rearrangement from cation oxygen to carbonium ion to take place, and thus to support the ionic mechanism.(3)

Hydroperoxides are among those materials which can decompose by either mechanism, depending on the conditions. Cumene hydroperoxide (CHP) is used as an initiator in the curing of GR-S rubbers, which is described as proceeding through a free radical chain reaction; the heat of vulcanization induces the decomposition of the CHP. (For convenience, the symbol "CHP" will be used for "cumene hydroperoxide"). The effect of metal salts on the rate of decomposition of CHP in styrene was studied by Fordham and Williams,(4) who note that the insignificant extent of polymerization suggests that the mechanism was ionic.

Seubold and Vaughan(5) postulated the following mechanism for the decomposition of CHP by strong acids:

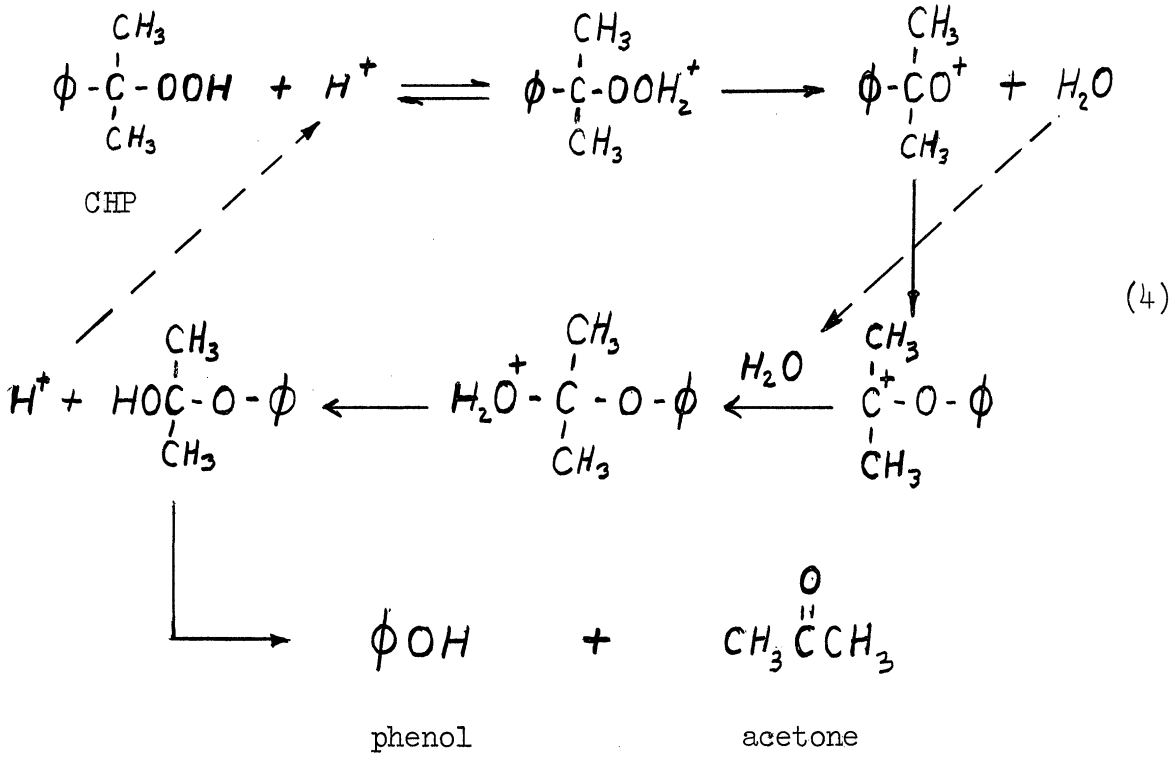

(4)

The appearance of water in the mechanism should be noted; water concentration was found to be an important variable in determining the rate, and it also appeared to affect the specificity of the reaction.

Seubold and Vaughan ran the reaction in acetic acid solution, in which CHP is stable at room temperature, with p-toluene sulfonic acid as the catalyst. The formation of the cationic oxygen intermediate is the key to the rearrangement which gives the final products, phenol and acetone. The greater ease of migration of the phenyl group as compared to the methyl group gives the high yield of the reaction, although some acetophenone resulting from methyl transfer is formed:

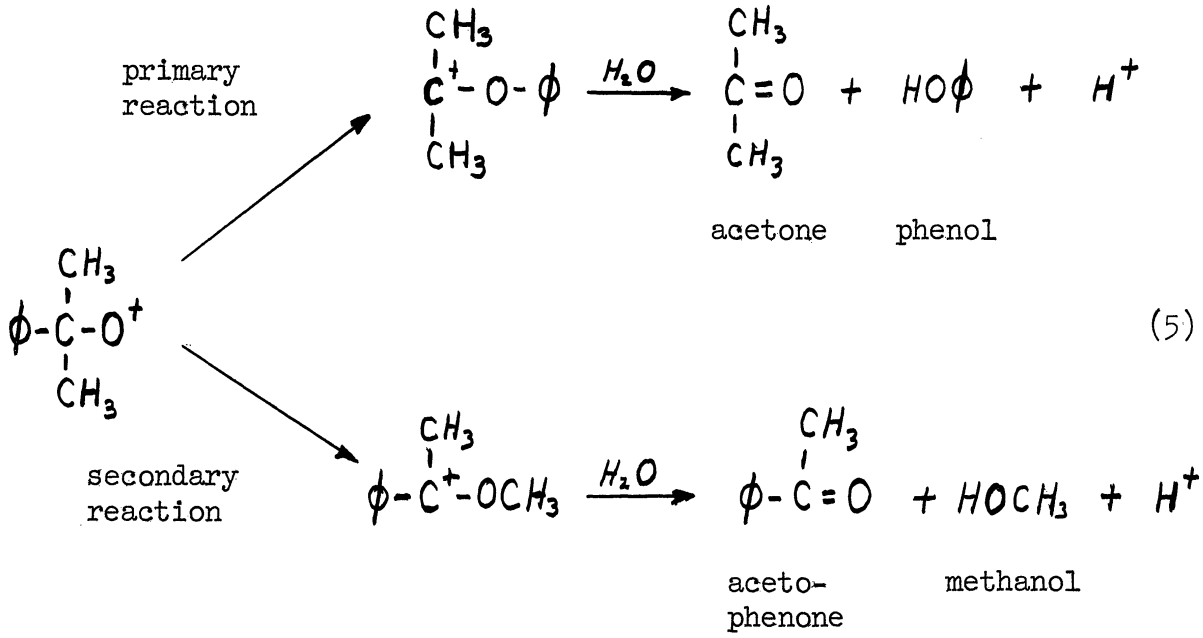

(5)

They report that the reaction is first order with respect to both CHP and hydronium ion. It was necessary to assume the order of the reaction in the derivation of the equation for correlation in this study on the basis of their work, so the range of their data is of interest. They

measured rates in batch experiments at two levels of CHP concentration (0.032-0.040 and 0.16-0.20 moles CHP/kg.) for each of three acid concentrations(0.05, 0.10 and 0.20 moles H_3O^+/kg.). A first order constant k_1 sec.$^{-1}$ resulted for each pair of CHP concentrations at a given acid concentration, and a constant k_2 kg. per (moles H_3O^+)(sec.), defined by

$$-\frac{d[CHP]}{d\theta} = k_2[H_3O^+][CHP] \qquad (6)$$

where

$$k_2[H_3O^+] = k_1$$

was determined to be independent of acid concentration.

Kharasch, Fono, and Nudenberg[6,7] studied the thermal- and acid-catalyzed decomposition of CHP and reported phenol, acetophenone, phenyl dimethyl carbinol, acetone, dicumyl peroxide, methane, methanol, water, ethylene, and hydrogen peroxide as products, with specific conditions determining the mechanisms which led to the various products. The strong acid-catalyzed reaction was quite specific, giving 90% yields of phenol and acetone.

The decomposition reaction is exothermic. An estimate of the heat of reaction ΔH is made from the heats of combustion of phenol, acetone, and CHP in the following manner:

$$C_6H_5C(CH_3)_2OOH\ (s) + 11\ O_2\ (g) \longrightarrow 9\ CO_2\ (g) + 6\ H_2O\ (l) + Q_c$$

$$Q_p + 3\ H_2O\ (l) + 6\ CO_2\ (g) \longleftarrow C_6H_5OH\ (s) + 7\ O_2\ (g)$$

$$Q_a + 3\ H_2O\ (l) + 3\ CO_2\ (g) \longleftarrow CH_3COCH_3\ (l) + 4\ O_2\ (g)$$

Adding these three equations gives

$$C_6H_5C(CH_3)_2OOH \longrightarrow C_6H_5OH + CH_3COCH_3 + Q_c - Q_p - Q_a$$

and $\Delta H = Q_p + Q_a - Q_c$. The values of the heats of combustion of phenol and acetone[8] at 20°C are

$$Q_p = 732.2 \text{ kg. cal./gm. mol.}$$

$$Q_a = 426.8 \text{ kg. cal./gm. mol.}$$

while the heat of combustion of CHP is reported[9] as

$$Q_c = 1219.6 \text{ kg. cal./gm. mol.}$$

The heat of reaction calculated from these values is $\Delta H = -60.6$ kg. cal./gm. mol. The reliability of the estimate is only fair, since it is calculated from the difference of large numbers, but it indicates that the reaction is exothermic to such an extent that temperature control in the catalyst bed is an important factor in experimental technique and temperature gradients may be important in interpreting the rate processes within the system.

The reaction goes essentially to completion, a 10% CHP solution having been decomposed in a high conversion run to 0.1% CHP. An order-of-magnitude estimate of the equilibrium constant likewise indicates that high conversion is possible; the equation

$$-RT \ln K = \Delta H - T\Delta S \qquad (7)$$

is applied with the calculated value of ΔH and an estimate of ΔS made as follows. Wenner[10] reports these entropy values at 25°C:

compound	S cal. per (mol.)(°C)
acetone (l)	47.9
phenol (s)	34.0
t-butylbenzene (l)	66.6

By the group substitution method,[11] using the entropy of t-butylbenzene as a basis, the entropy of CHP can be estimated to be between S_I = 58.4 cal. per (mol.)(°C) and S_{II} = 67.8 cal. per (mol.)(°C) where

I is 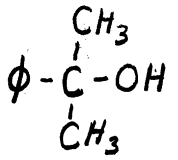 and II is 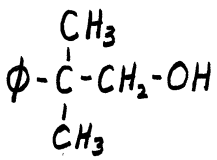

Taking the non-conservative upper limit S_{CHP} = 67.8 cal. per (mol.)(°C) as the estimate, the entropy change of the reaction is calculated to be positive:

$$\Delta S = S_{acetone} + S_{phenol} - S_{CHP} = 14.1 \text{ cal. per (mol.)(°C)}$$

Thus from Equation (7)

$$\ln K = \frac{-(60{,}000 + \mathcal{C})}{-(1.98)(298)} > 100$$

and

$$K > 10^{44}$$

Actual operating conditions were far from equilibrium, so the rate of the reverse reaction was assumed negligible in setting up a mathematical model. On the basis of the work of Seubold and Vaughan the reaction was also assumed first order in both CHP and hydronium ion; the necessity of the assumption is shown later. These two assumptions are expressed by the equation

$$R = -\frac{d[CHP]}{d\theta} = k_2[H_3O^+][CHP] \qquad (8)$$

where the rate is in moles CHP per (min.)(cm.^{3}), the concentrations are in moles per cm.^{3} and k_2 has the units cm.^{3} per (min.)(mole H_3O^+).

The Nature of the Catalyst

Ion exchange resins are materials which have functional groups capable of ionizing attached to polymeric substances which are insoluble in the medium with which exchange is to take place. Some naturally occurring materials have the properties of ion exchange resins, but synthetic resins containing only one type of functional group are usually more useful because they are more specific in their action. Both acid and basic exchange resins are made, the functional groups of the acid or cation exchange resins being carboxylic, sulfonic, and phenolic. The strength of the different acid groups in the resin is comparable to the strength of that group on simple structures, as has been determined by Topp and Pepper.[12] They ran titration curves on mono- and polyfunctional resins which showed that $-SO_3H$ resins are strong acids; $-CO_2H$ resins, weak acids; and -OH (phenolic) resins, very weak acids. The polyfunctional resins gave curves of intermediate forms indicating that the various groups function independently of each other. The method of titration provides a simple and rapid method of determining the capacity of the resin, that is, the equivalents of ionizing groups per unit weight.

Several conditions must be met for the resins to be useful catalysts: the resin structure must be stable in the reaction environment; the reactants and products must be able to diffuse through the resin to and away from the acid groups; and no exchange with the reaction environment which might destroy the acid character of the functional groups can occur.

The fact that a strong acid is required to catalyze the decomposition of CHP to phenol and acetone dictates the use of an ion exchange resin with sulfonic acid groups. Dowex 50, made by Dow Chemical Company, is such a resin. It is made by polymerizing styrene with varying percentages of the cross-linking agent divinylbenzene, followed by sulfonation with H_2SO_4, which introduces sulfonic acid groups on the aromatic rings. The result is the gel structure indicated in Figure 1, page 12. The actual structure is a three dimensional network of substituted methylene chains connected by aromatic ring cross-links. The acid groups are thus spread fairly uniformly through the resin structure. The gel structure results in the resin being insoluble in organic liquids. Bauman and Eichhorn,[13] listing the fundamental properties of Dowex 50, give the capacity of the oven-dry resin as 4.92 milliequivalents of acid per gram and the internal concentration as 3.5 moles of acid per liter of resin. The resin is in the form of spherical particles from 20 to 200 mesh in diameter. Besides size, the most important variable for a sample of resin is the degree of cross-linking, and it is important to note that, for a given degree of cross-linking, properties such as capacity for exchange or swelling, when expressed on a weight basis, are independent of particle size, indicating the uniformity of the resin structure.

The gel structure of the resin permits absorption of liquids into the interior of the particles, with both absorption and desorption of small molecules being rapid. Sundheim et al.[14] measured the weight of water absorbed from air as a function of humidity and found a slight ($\pm$ 2½% maximum) but reproducible hysteresis on an absorption-desorption cycle,

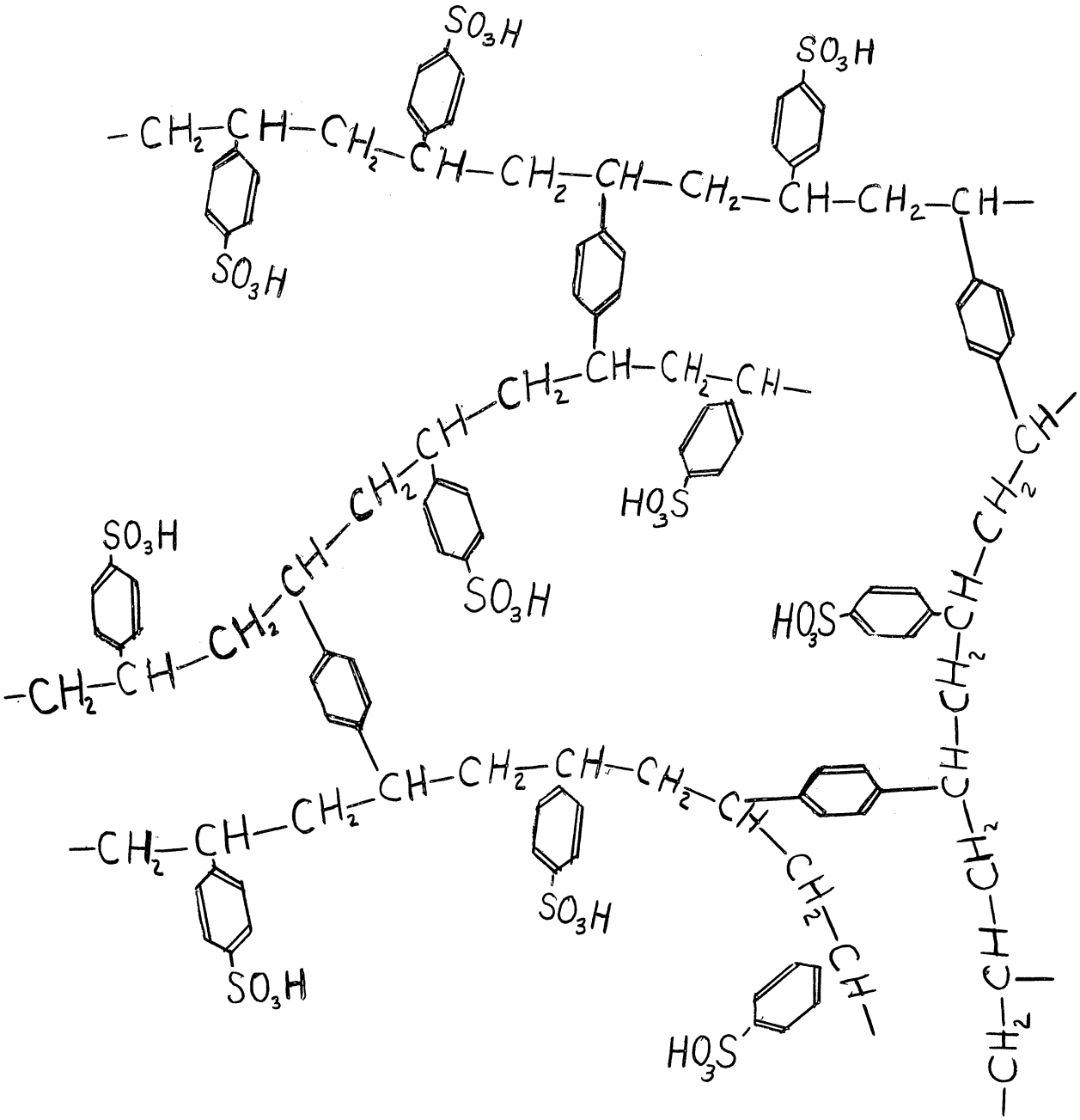

Figure 1. Representation of Catalyst Gel Structure.

indicating that the distribution is not exactly an equilibrium state. The liquid absorbed causes the particles to swell; the increase in volume is only slightly smaller than the volume of the liquid absorbed, and the particle in the swollen state is interpreted as having a continuous internal liquid phase. Theories of swelling assume that, at equilibrium, osmotic pressure and pressure from ion hydration are balanced by the stresses in the polymer network.(15)

The effect of increased cross-linking is to tighten the resin network and therefore to reduce absorption and swelling. The degree of cross-linking also affects the phase distribution coefficients (defined and discussed below), the rates of exchange and diffusion, and the effective exchange capacity for large organic ions.(16) The latter indicates that there is a limit to the size of molecule which can diffuse through the gel structure. This has been noted by others: Richardson(17) used ion exchange resins to separate inorganic ions from dye ions and found that the quantity of dye absorbed depended on its size. Dye ions of 30 Å diameter were unable to penetrate the gel structure. For dye ions of 15 Å diameter, only 5% of the resin capacity was used and for dye ions of 10 Å diameter, 94% of the resin capacity was used.

Hale et al.(18) performed experiments with resins of different degrees of cross-linking and found that the rate of absorption of Zn^{++} from acridine orange-ZnCl solution was lower using resin of 10% cross-linking than the rates for resins of 5 and 15% cross-linking. The interpretation given was that the 5% cross-linked network was loose enough to

permit the dye to absorb freely with the zinc ion, while the 15% cross-linked network was tight enough that only the zinc ion diffused in; for the 10% cross-linked network the diffusion of the dye ions occurred, but it was hindered by the network, and this interferred with the zinc ion diffusion by blocking the network openings. This illustrates how the use of an ion exchange resin as a catalyst is dependent on the ease with which the reactants and products can diffuse through the network. For reactions involving large molecules, selection of a low cross-linked resin might give successful catalysis where more highly cross-linked resin would not. Changing the degree of cross-linking may not affect the diffusion rate of small molecules, since the resistance to diffusion is the internal liquid phase, not the size of the network openings.

The property of absorbing some components from a multicomponent mixture in preference to others results in concentration differences between the external liquid phase and the absorbed liquid phase within the resin. This can be described by phase distribution coefficients, which are defined as the ratios of the internal concentrations to the external concentrations. At first the phenomenon was considered as a molecular absorption process,[19,20,21] although it was noted to be a volume rather than a surface effect. Workers in ion exchange then came to consider it as a phase equilibrium phenomenon, examples being the selective absorption of water from HCl-water solution[16] and the distribution of uncharged (non-ionizing) organic molecules. Reichenberg and Wall[22] studied the effect of cross-linking and found that the phase distribution coefficients changed as the degree of cross-linking changed. Davies and Owen[23] found that 0.9

mole fraction acetone (in water) outside 10% divinylbenzene resin gave 0.16 mole fraction acetone inside at equilibrium.

Phase distribution coefficients were not considered in much of the work in which the resins were used as catalysts. Boyd et al.[24] derived equations for non-steady state reaction with film, diffusion, and chemical control in which they included a distribution coefficient. They assumed that it was independent of concentration and it cancelled out of their final equations. For their work with trace absorbents the assumption was valid, but later workers applied their equations in regions in which they were not valid.[25] Smith and Amundsen[26] derived equations for continuous reaction systems, with no consideration of distribution coefficients; their equations were also applied subsequently by other workers. A number of people[27,28,29] compared reaction rates in the resin with rates in homogeneous mineral acid solutions, defining an efficiency as the ratio of the rate using the resin as catalyst to the rate in homogeneous solution. Noting the decline of this efficiency with increasing chain length in the hydrolysis of a homologous series of esters, Bernard and Hammett[30] found it necessary to correlate the rates of hydrolysis of the esters RCO_2CH_3 with the entropy of the corresponding hydrocarbon RH, this being the only property they found which gave correlation. Finally, Helfferich[31] noted that phase distribution effects would explain their results; he defined a phase distribution coefficient, which he expected to be independent of concentration, and suggested its inclusion in Smith and Amundsen's work.

Saletan[32] and Barker[33] used phase distribution coefficients in describing their studies, both of which were similar in nature to this study. Both assumed that the phase distribution coefficients were independent of composition and temperature. They measured them by immersing oven dry resin in the pure liquid and observing the increase in the resin volume due to the absorbed liquid. The moles of liquid absorbed and the final volume of the resin phase gave them a resin phase concentration; the density of the pure liquid gave them a liquid phase concentration; and the ratio of resin phase concentration to liquid phase concentration gave them a phase distribution coefficient, which was necessarily less than one. They considered the resin structure as a part of the "homogeneous" resin phase.

A different concept is applied in the present study. The concentrations in the absorbed liquid within the resin phase are referred to the volume of the absorbed liquid only. Thus the phase distribution coefficient for a pure liquid would be unity. If the phase distribution coefficient as defined in this manner were not a function of composition, there would be no difference in composition between the absorbed liquid and the external liquid. The data of Davies and Owen[23] for the system acetone-water show that there is a difference, with a strong preference for water absorption found. Conversion of their data to the basis used by Saletan and Barker shows that their phase distribution coefficient is also a function of composition.

The method of Davies and Owen is suitable only for measuring phase distribution coefficients in a non-reacting system. In a reacting

system, the reaction changes the components and thus negates a material balance.

Derivation of the Mathematical Model

The rate of reaction as a function of the reaction environment must be estimated from measurements of finite changes in composition over finite time intervals. In a flow reactor, the rate of reaction R of a component j is determined from steady-state values of initial and final composition, C_{ji} and C_{jf}; flow rate, W; and reactor volume, V, or some other measure of reacting space.

The value of R calculated from steady-state values of C_{ji}, C_{jf}, W, and V is an average value taken as an estimate of the rate at the average value of parameters such as temperature, flow rate, composition, etc., which existed in the reactor at steady state. Theoretically, the reactor could be operated so that the differences between input and output become differential in size and an instantaneous or point rate measured. In practice, experimental error in composition measurement requires operating the reactor to obtain a finite difference between input and output compositions which is significantly larger than the experimental error. Under such conditions, the point rate usually varies through the bed; a mathematical model of the processes occurring is used to relate the calculated (average) rate to the average parameter values.

The equations for describing the rate process were derived on the following interpretation of the steady state condition. The overall process proceeds by diffusion of the cumene hydroperoxide from the liquid

phase to the acid sites in the resin phase, where the reaction takes place, followed by diffusion of the products back into the liquid phase. It is assumed that the liquid flow rate can be made high enough that resistance to diffusion in the liquid phase is negligible, i.e., no concentration gradient for the reacting component exists in the liquid phase; that the concentrations of CHP in the two phases at the surface can be related by defining a phase distribution coefficient λ which is a function of liquid phase composition; that the reaction proceeds by a mechanism first order in CHP concentration with the rate of the reverse reaction insignificant; and that the resulting CHP gradient within the particle is a function of radius only, with the catalyst particles being spherical.

Consider a spherical element of a catalyst particle (Figure 2, page 19) at radius x and of thickness dx. With the direction of increasing x considered positive, the areas of the inner and outer surfaces are designated as A and A + dA cm.^{2} respectively; likewise the rates of CHP diffusion are w and w + dw mol. CHP per (min.)(cm.^{2}) and the rates of heat transfer are q and q + dq cal. per (min.)(cm.^{2}). Writing a material balance on the CHP, the difference between the inlet and outlet diffusion rates must be equal to the rate of decomposition by reaction within the element:

in (diffusion) - out(diffusion) = out (reaction)

or

$$wA - (w + dw)(A + dA) = R_x A\, dx \qquad (9)$$

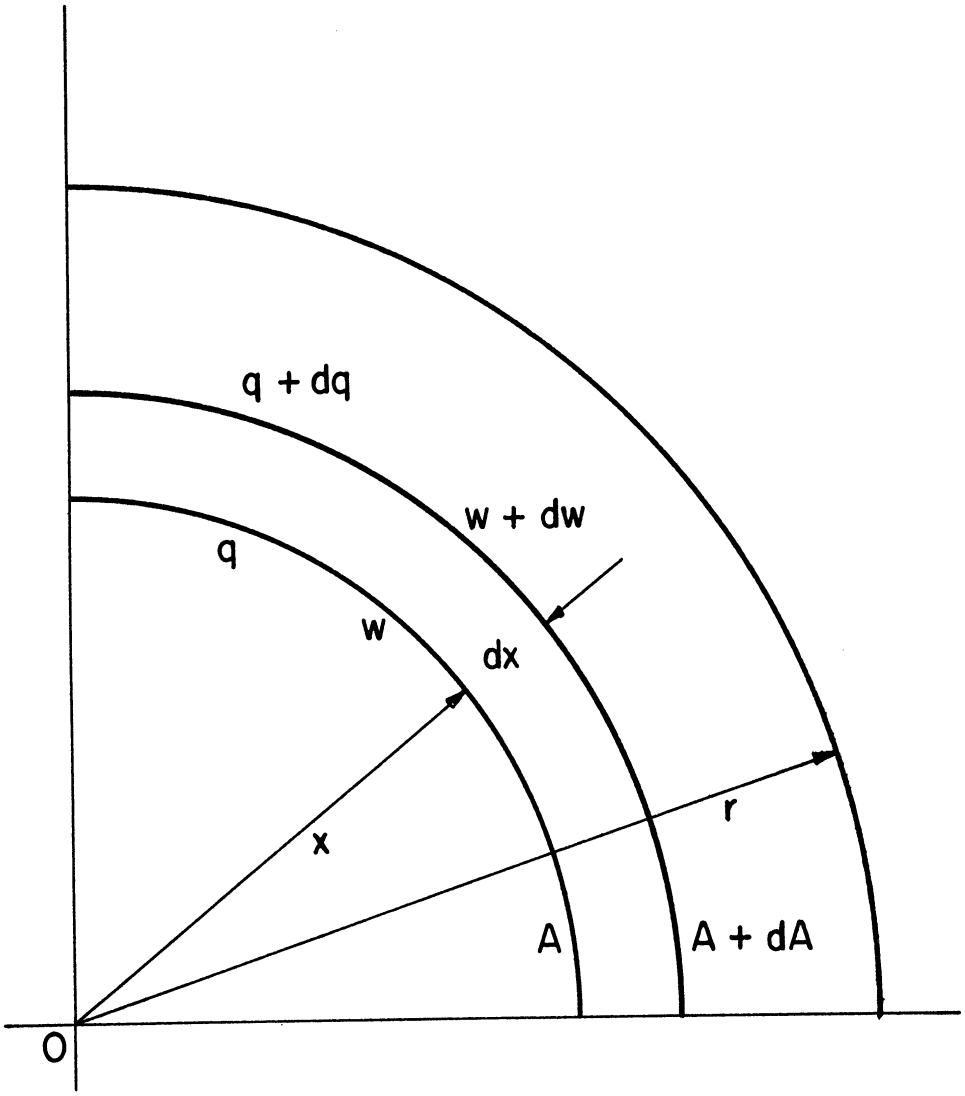

Figure 2. Spherical Element in Catalyst Particle.

The subscript x on R indicates that R is a function of position x in the particle; the units of the variables: w mol. CHP per (min.)(cm.^{2}); A cm.^{2}; R_x mol. CHP decomposed per (min.)(cc.); and x cm. All of the variables are functions of x. Expressing the areas as functions of x gives:

$$4\pi w x^2 - 4\pi(w + dw)(x^2 + 2x\,dx) = 4\pi R_x x^2 dx \qquad (10)$$

Expanding, dividing by $4\pi dx$, and neglecting the second order differential gives

$$-2xw - x^2\left(\frac{dw}{dx}\right) = R_x x^2 \qquad (11)$$

In order to reduce Equation (11) to a function of composition and radius only, the forms for w and R_x as functions of composition must be assumed. The rate of diffusion w is expressed as a function of the composition gradient by

$$w = -D\frac{dC'}{dx} \qquad (12)$$

D is the diffusivity of CHP, cm.^{2}/min. The symbol C' stands specifically for the concentration of CHP in the resin phase, mol. CHP/cm.^{3} (External phase concentrations are indicated by C_j, with the appropriate subscript being used). D is assumed not to be a function of x. Differentiating (12) with respect to x on this basis gives

$$\frac{dw}{dx} = -D\frac{d^2C'}{dx^2} \qquad (13)$$

Expressing R_x as some function of C' is equivalent to assuming the order of the reaction. It should be noted that it is not possible to measure the order of the reaction with this catalyst. The reaction takes place in the resin phase and the compositions in that phase cannot be measured; the values of the phase distribution coefficient λ, defined as the ratio of the resin-phase composition C' to the liquid-phase composition C_c, are therefore unknown, and the functional relationship between C_c and λ cannot be determined. The order of the reaction would normally be measured by determining a constant c_1 independent of concentration C' by fitting the data to an equation of the form

$$R = c_1 (C')^n$$

where n would be taken as the order of the reaction. Since C' is known only by $C' = \lambda C_c$

$$R = c_1 (\lambda C_c)^n$$

But λ is an unknown function of C_c ; say $\lambda = f(C_c)$, so that

$$R = c_1 [f(C_c) \cdot C_c]^n$$

and a pseudo-order n' would result from fitting the data to an equation of the form

$$R = c_2 (C_c)^{n'}$$

An order of the reaction is thus assumed in the further derivation of the mathematical model, and experimental deviations from this order are interpreted as variations in the phase-distribution coefficient. Since this

catalyst gave the same high yield of phenol as the homogeneous reaction which was determined to be first order in CHP and hydronium ion, it was assumed that the reaction was proceeding by the same mechanism. The assumption of first order was expressed by Equation (8), page 9. The notation of the equation is modified for use in the model derivation. The acid concentration is assumed not to be a function of radius, that is, the catalyst particle is uniform. The rate constant k_1 min.$^{-1}$ is therefore substituted for the product $k_2[H_3O^+]$. The concentration of interest is that in the resin phase, so C' mol. CHP/cm.^{3} is substituted for [CHP]. Finally, the rate at radius x is indicated by R_x:

$$R_x = k_1 C' \tag{14}$$

Substituting Equations (12), (13), and (14) into Equation (11) gives

$$2D\frac{dC'}{dx} + xD\frac{d^2C'}{dx^2} = k_1 C' x$$

which is rearranged to

$$x^2\frac{d^2C'}{dx^2} + 2x\frac{dC'}{dx} - \frac{k_1}{D}x^2C' = 0 \tag{15}$$

Equation (15) gives the concentration of CHP within the particle as a function of the radius with a single parameter, the ratio of the chemical reaction rate constant to the diffusivity of CHP in the resin phase.

Since the reaction being studied is exothermic, it is necessary that the center of a catalyst particle be warmer than the surrounding

liquid to provide a gradient for removing the heat of reaction. If the magnitude were great enough, this increased temperature could have a significant effect on the rate of reaction. Both k_1 and D are expected to increase with temperature, so the ratio is not as sensitive to temperature change as k_1 alone is. An energy balance is presented in Appendix B showing that the temperature rise within the particle is expected to be less than 1°C, and Equation (15) is solved on the basis that k_1/D is constant.

Let $k_1/D = \alpha^2$ cm.$^{-1}$ Then Equation (15) is a generalized Bessel equation with the solution:(34)

$$C' = (x)^{-\frac{1}{2}} \left[a_1 I_{\frac{1}{2}}(\alpha x) + a_2 I_{-\frac{1}{2}}(\alpha x) \right] \qquad (16)$$

where a_1 and a_2 are unknown constants. Equation (16) may be expressed in hyperbolic functions:

$$C' = \frac{1}{x}\sqrt{\frac{2}{\pi\alpha}} \left[a_1 \sinh(\alpha x) + a_2 \cosh(\alpha x) \right] \qquad (17)$$

The boundary conditions for determining the constants are

(1) $C' = C'_s$ at $x = r$

(2) $(dC'/dx) = 0$ at $x = 0$

that is, the concentration of CHP at the particle surface in the resin phase is designated by C'_s and there is no concentration gradient at the center of the particle.

Differentiating Equation (17) with respect to x gives

$$\frac{dC'}{dx} = -\frac{1}{x^2}\sqrt{\frac{2}{\pi\alpha}}\left[a_1 \sinh(\alpha x) + a_2 \cosh(\alpha x)\right] + \frac{\alpha}{x}\sqrt{\frac{2}{\pi\alpha}}\left[a_1 \cosh(\alpha x) + a_2 \sinh(\alpha x)\right] \tag{18}$$

Using boundary condition (2) in Equation (18):

$$0 = \sqrt{\frac{2}{\pi\alpha}}\left[a_1 \sinh(0) + a_2 \cosh(0)\right] + 0$$

from which $a_2 = 0$, since $\sinh(0) = 0$, $\cosh(0) = 1$. $a_2 = 0$ is substituted into Equation (17) and boundary condition (1) applied:

$$C_s' = \frac{1}{r}\sqrt{\frac{2}{\pi\alpha}}\left[a_1 \sinh(\alpha r)\right]$$

from which

$$a_1 = \frac{r\, C_s'}{\sinh(\alpha r)}\sqrt{\frac{\pi\alpha}{2}}$$

The solution to Equation (15) is thus

$$C' = C_s' \frac{\alpha r \cdot \sinh(\alpha x)}{\alpha x \cdot \sinh(\alpha r)} \tag{19}$$

and the concentration C' at the point x is the indicated function of particle size r, surface concentration C_s', and the parameter $\alpha = (k_1/D)^{\frac{1}{2}} cm^{-1}$.

The overall rate R for a particle is an integrated average of the point rate R_x. Thus:

$$R = \frac{4\pi \int_0^r R_x x^2 dx}{\frac{4}{3}\pi r^3} = \frac{3}{r^3}\int_0^r R_x x^2 dx \tag{20}$$

Combining Equation (14) (chemical rate equation) and Equation (19) (concentration as a function of radius) gives

$$R_x = k_1 C_s' \frac{\alpha r \cdot \sinh(\alpha x)}{\alpha x \cdot \sinh(\alpha r)} \tag{21}$$

which is the point rate as a function of radius x for a given surface concentration C_s'; this is substituted into Equation (20):

$$R = \frac{3}{r^3} \int_0^r k_1 C_s' \frac{\alpha r \cdot \sinh(\alpha x)}{\alpha x \cdot \sinh(\alpha r)} x^2 dx \tag{22}$$

The variable of integration is changed to αx:

$$R = \frac{3 k_1 C_s'}{\alpha^2 r^2 \sinh(\alpha r)} \int_0^{\alpha r} (\alpha x) \sinh(\alpha x) d(\alpha x) \tag{23}$$

This integrates to

$$R = 3 k_1 C_s' \left[\frac{\alpha r \cosh(\alpha r) - \sinh(\alpha r)}{\alpha^2 r^2 \sinh(\alpha r)} \right] \tag{24}$$

The form of the equation is seen to be similar to the original chemical rate Equation (14). The terms involving particle size r are taken to define a dimensionless efficiency factor ϕ:

$$\phi = 3 \left(\frac{\alpha r \cosh(\alpha r) - \sinh(\alpha r)}{\alpha^2 r^2 \sinh(\alpha r)} \right) \tag{25}$$

which gives the rate for a particle as

$$R = k_1 \phi C_s' \quad \frac{\text{mol. CHP decomposed}}{(\text{min.})(\text{cc.})} \tag{26}$$

The average rate remains first order in C_s' with the addition of the efficiency factor ϕ.

The importance of ϕ depends on the magnitude of the product αr. For a given particle size, as $\alpha \rightarrow 0$, $\phi \rightarrow 1$, which means that diffusion is rapid compared to the chemical rate (D is greater than k_1 and therefore $\alpha = (k_1/D)^{\frac{1}{2}}$ is small), and the catalyst is being used effectively. As α increases (for fixed r), $\phi \rightarrow 0$, and the catalyst is not being used effectively; the efficiency ϕ could be increased by using a smaller particle size.

If the particle size is an important factor in determining the rate, the process is sometimes spoken of as being diffusion controlled, while if the rate is independent of particle size the phrase "chemically controlled" is applied. This can lead to confusion, since these same terms are used to distinguish processes of different activation energies, low activation energies being ascribed to diffusion controlled processes and high activation energies to chemically controlled processes. In the present study, a dependence on particle size is combined with a high activation energy, giving contradictory descriptions from the two classifications. Both diffusion and the chemical rate combine to determine the actual rate in this catalyst, and no attempt is made in this report to proportion the control between the two processes.

In a packed bed flow reactor, a material balance on the reacting component can be written around the element dn (See Figure 3) in terms of input and output by flow and output by reaction:

$$\frac{W C_c}{\rho} - \frac{W}{\rho}(C_c + d C_c) = \frac{R}{m} dn \qquad (27)$$

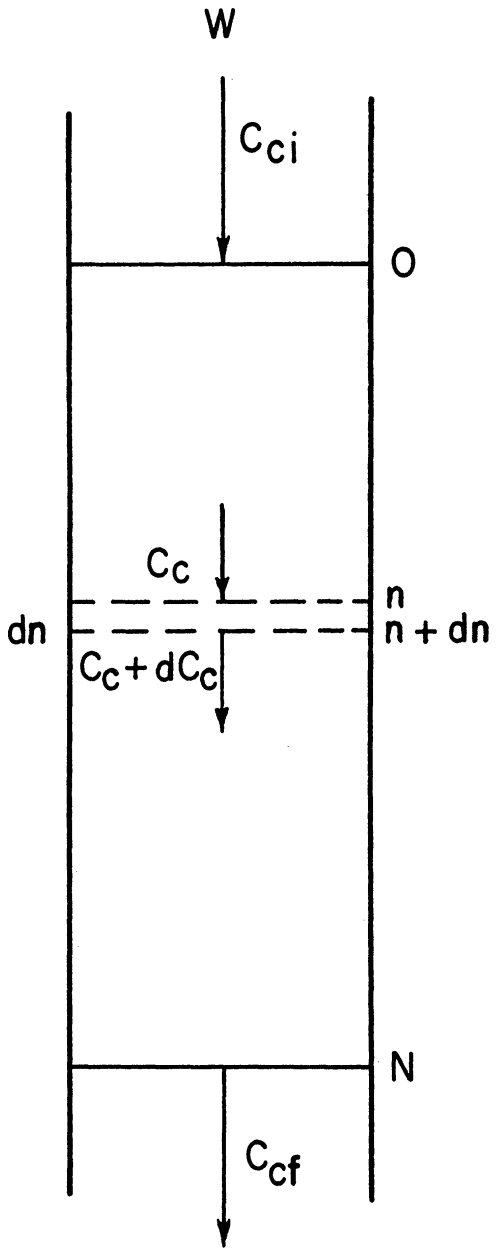

Figure 3. Differential Element of Catalyst in Reactor.

The variables are W, flow rate, gm./min.; C_c, concentration of CHP, mol. CHP/cm.^{3}; ρ, liquid density, gm./cm.^{3}; m, equivalents of acid per cm.^{3} of catalyst; R, average reaction rate of particle, moles CHP per (min.)(cm.^{3}); and dn, equivalents of acid in the element. ρ and m are considered constant through the length of the reactor. Substituting for R from Equation (26) gives, with rearranging,

$$dn = -\frac{W}{k_1 \phi}\left(\frac{m}{\rho}\right)\frac{dC_c}{C_s'} \tag{28}$$

C_s' can be related to C_c by the definition of the phase distribution coefficient and the assumption that there is no concentration gradient in the liquid phase (C_{cs} is the CHP concentration at the surface of the liquid phase):

$$C_s' = \lambda C_{cs} \tag{29}$$

$$C_{cs} = C_c \tag{30}$$

These equations are substituted successively into Equation (28):

$$dn = -\frac{W m}{k_1 \phi \lambda \rho}\frac{dC_c}{C_c} \tag{31}$$

This is integrated to give the relationship between flow rate W, bed size in equivalents N, and initial and final concentrations of CHP C_{ci} and C_{cf}:

$$N = \frac{W m}{k_1 \phi \lambda \rho} \ln \frac{C_{ci}}{C_{cf}} \tag{32}$$

Rearranging, a variable k gms. per (min.) (equivalents H^+) is defined which is calculated from a given set of steady state values for N, W, C_{ci}, and C_{cf}:

$$k = \frac{k_1 \phi \lambda \rho}{m} = \frac{W}{N} \ln \frac{C_{ci}}{C_{cf}} \qquad (33)$$

Variation in k with the parameters temperature, particle size, and composition are interpreted in terms of variation in k_1, ϕ, and λ respectively, ρ and m being considered constants.

EQUIPMENT

The equipment was designed and constructed so that constant values of flow rate, feed composition, and bed temperature could be maintained to give a steady-state output composition. A diagrammatic sketch of the equipment is given in Figure 4, page 31. The sequence of units in the flow system was a feed tank, deaerator, Milton Roy simplex pump, pressure gauge, air bleed side stream with valve, and the reactor unit, with auxilliary equipment of a constant temperature water tank and circulating pump to provide temperature control. The feed pump and connecting tubing to the top of the reactor were type 304 stainless steel; the remainder of the system including the reactor was glass, 7 and 12 mm tubing, with polyethylene joints connecting the units. A corrosion-resistant system was desirable for two reasons. Since the catalyst was a strong acid, contact with non-resistant metals would have resulted in both corrosion of the equipment and catalyst deactivation. Likewise, ions from corrosion in any part of the system could exchange with the catalyst and thus deactivate it.

The feed tank, a 1000 cc graduated cylinder, was elevated to provide a positive pressure through the deaerator to the suction side of the pump. The line leaving the feed tank was constricted sufficiently to hold an air bubble in the line. The air bubble prevented the material in the line from rising into the feed tank and thus changing the composition of the feed. The deaerator consisted of a 10-inch bed of 60-mesh glass

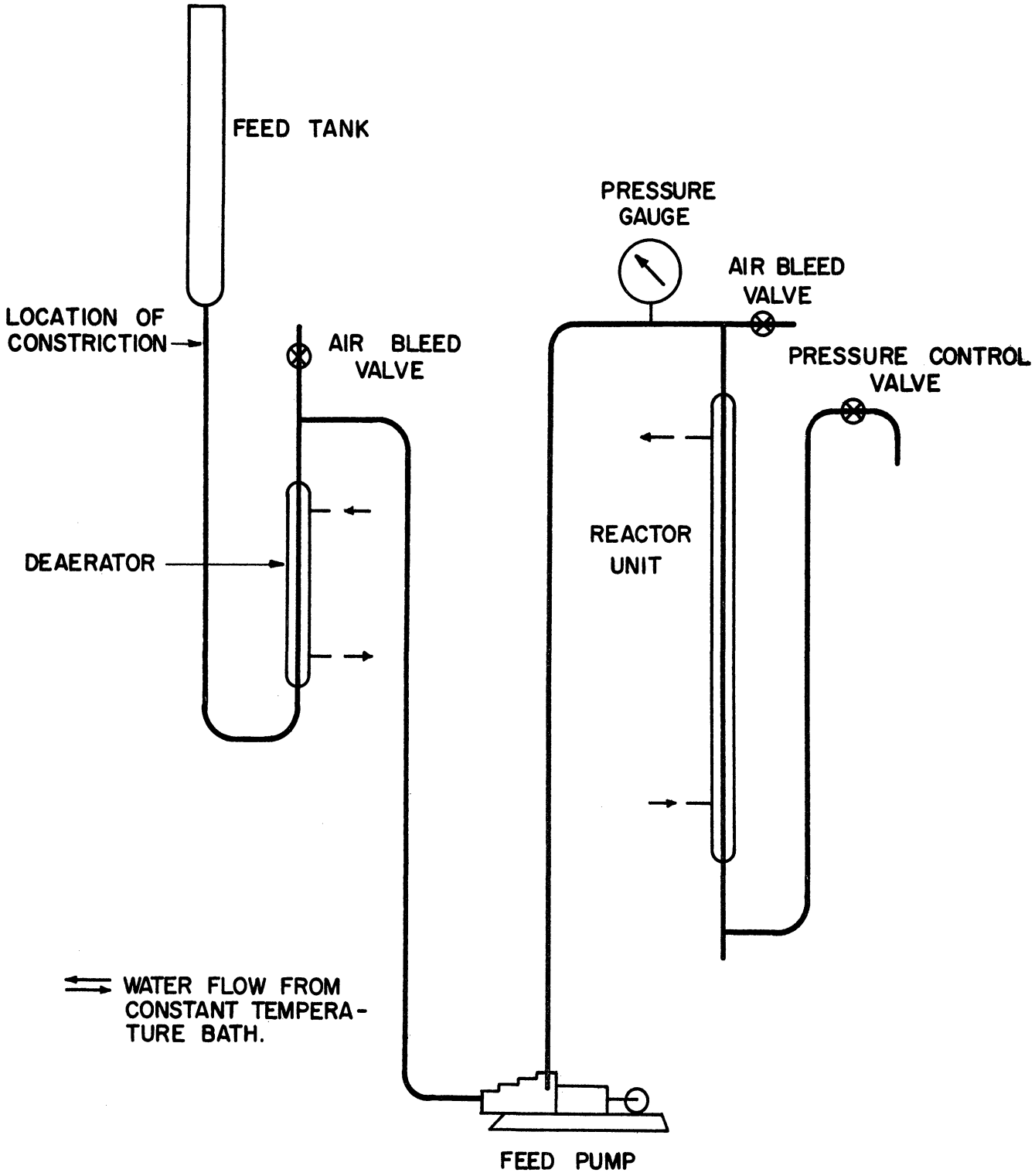

Figure 4. Diagrammatic Sketch of Equipment.

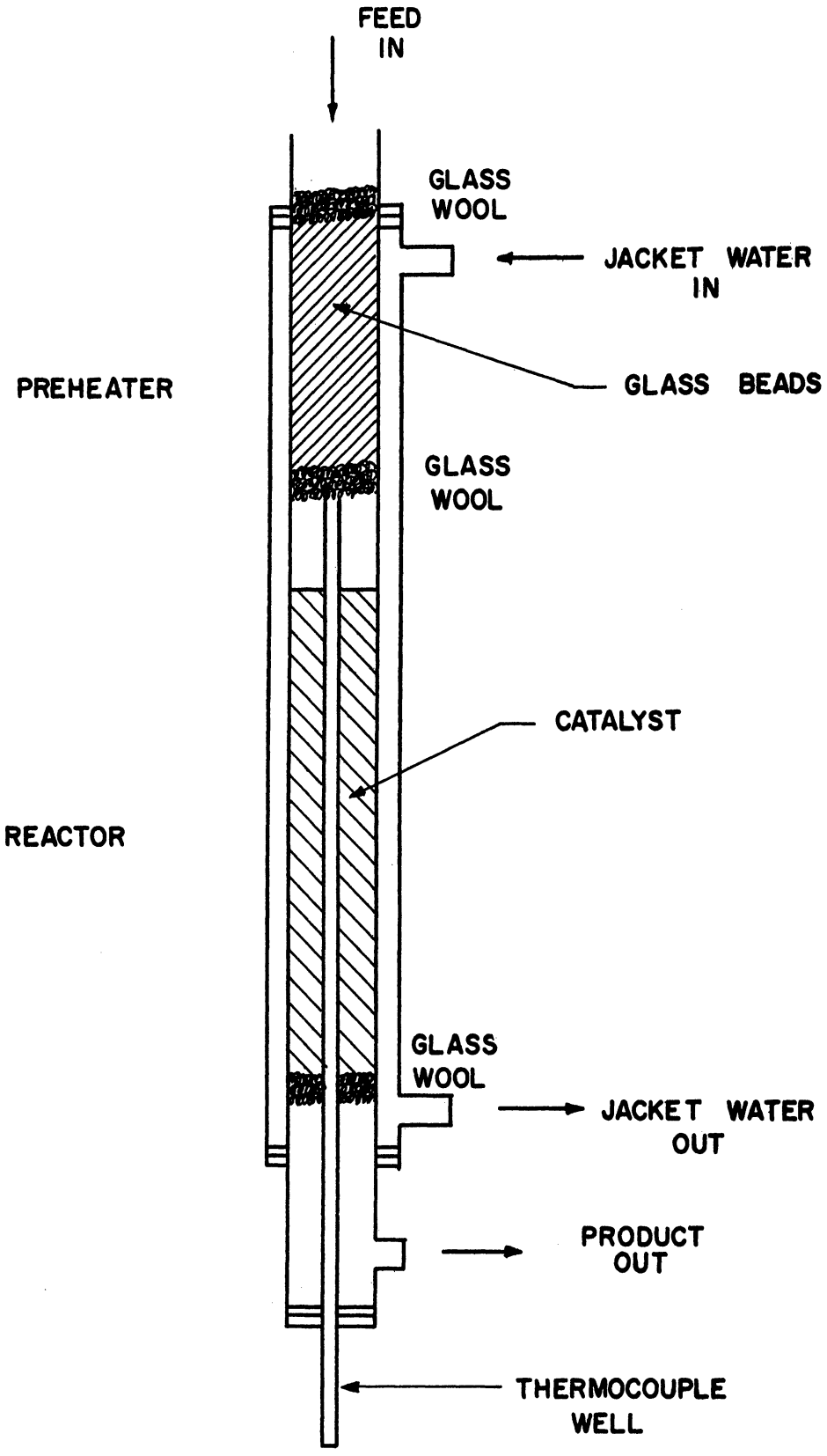

Figure 5. Cutaway View of Reactor Unit.

beads supported on glass wool in a jacketed section of 12 mm tubing. The feed passed upward through the glass beads, being heated by water circulated from the constant temperature tank, with dissolved air coming out as a result of the heating. Collected air was bled intermittently from the top of the deaerator while the feed passed by a side arm down to the pump. Deaeration was necessary to prevent air bubbles from forming in the catalyst bed during a run and thus changing the flow pattern.

The reactor unit, constructed of 12 mm tubing with a jacket of 18 mm tubing, consisted of a preheater and the catalyst bed operated in sequence in downflow (Figure 5, page 32). The preheater was a 10-inch section of 60-mesh glass beads held in place with glass wool plugs. The catalyst particles were supported on a glass wool plug in the annulus between the 12 mm tubing and a 5 mm tubing thermocouple well inserted from the lower end of the reactor. The upper end of the catalyst bed was not restricted by glass wool; expansion and contraction of the bed occurred with changes in environment, and some free space was left above the bed to permit it to remain in a loosely settled form. The thermocouple well was open at the lower end to permit measurement of longtitudinal temperature distribution in the bed during operation with a sliding thermocouple. A pinchcock on the outlet from the reactor unit was used to keep the pressure in the bed high enough that no air bubbles could form.

Water from the constant temperature tank was circulated through the jacket of the reactor unit to control the bed temperature at the desired level. A continuous record of the thermocouple readings in the bed

or the tank could be made on a Micromax recorder-indicator to observe non-steady state operation. Actual measurements of the two thermocouple voltages were made with a Leeds and Northrup potentiometer. A single thermocouple was used for both locations, and its calibration was checked occasionally in the constant temperature tank against a calibrated thermometer. An open steam line and a 500 watt Calrod heater connected by relay to a Fenwal Thermoswitch maintained the temperature in the tank and provided control to ± 0.25°C.

The flow rate was adjusted by varying the stroke length on the Milton Roy pump. Being a single piston pump, it introduced the feed in pulses; at the flow rates of interest (less than $7\frac{1}{2}$ cc per minute), the resistance of the preheater and the expansion of the system between the pump and the preheater flattened the pressure pulse so that essentially smooth flow was observed to exist after the preheater, the system being tested with no catalyst charge in place. A given setting of the pump stroke delivered feed with a variation in average rate (timed over one minute intervals) of about 1%. The flow rate was measured by timing the collection of a known volume of the total output and converting this to a weight rate with a density measurement.

To insert a new catalyst charge the reactor unit was removed from the system. The old catalyst was washed out the bottom, the thermocouple well reinserted with a fresh glass wool plug at the upstream end, and the reactor unit filled with acetone containing 8-10% water. This ensured that the catalyst settled in an expanded or swollen state while

providing a convenient technique for assuring complete transfer. The catalyst then was added, followed by a glass wool plug, with 2-3 inches of free space left for expansion. The opening was stoppered and the reactor unit replaced in the flow system. For measurement of the experimental variable k at high reaction rates (k greater than 25 grams per (minute) (equivalents H^+) at 10% CHP), the catalyst was diluted with 60-mesh glass beads to reduce the heat released per unit length and thus keep the temperature rise of the bed from the exothermic reaction at a negligible value. The total acidity of the catalyst charge was calculated from the weight of resin added and its specific capacity. The latter was measured for each sample of resin by titration of a weighed sample in NaCl-saturated water with standard NaOH. The salt exchanged with the acid groups, converting them to salt form and freeing the acid for titration. The capacity of the resin was calculated from the volume of NaOH used, its normality, and the weight of the resin sample, and was expressed as milliequivalents of acid per gram of catalyst.

Most of the air in the reactor unit was bled out the relief valve by feeding acetone backwards through the system with air pressure. The air remaining in the bed and preheater after this was dissolved by the feed stream as part of the start-up procedure of the next run.

MATERIALS

The Dowex 50 supplied by Dow Chemical Company for use as catalyst is a sulfonated polystyrene resin cross-linked with divinylbenzene. Sulfonation introduces sulfonic acid groups in the para position of the aromatic rings which give reactions indicating that they function as strong acids. The cross-linking agent gives a gel which is insoluble in solvents which dissolve polystyrene.

The following samples were received:

Dowex 50 X 8 (8% divinylbenzene)

20-50 mesh
50-100 mesh
100-200 mesh

Dowex 50 X 4 (4% divinylbenzene)

50-100 mesh

Dowex 50W X 8

20-50 mesh

The latter differs from the others in being lighter in color and mechanically stronger. All but one sample was received in hydrogen form; this one was converted from sodium to hydrogen form by washing with hydrochloric acid until the acid showed no sodium in a flame test, then washing with distilled water until the wash was neutral. All samples were dried to equilibrium at 70°F and 50% relative humidity and size ranges of 32-35, 60-65, and 115-150 mesh were screened from the appropriate sample with standard sieves. These size ranges have average diameters in

the ratio of 4:2:1, respectively, and are subsequently designated as large, medium, or small, or (L), (M), or (S). The resin has the property of swelling or shrinking in response to changes in external environment; for example, the air-dry resin expands by a factor of 1.57 in volume when submerged in acetone. This property must be taken into account in comparing one experimental condition to another when particle radius is important.

The particles of all samples were spherical except for the 50 X 8 32-35 mesh sample; breakage had resulted in half-spheres and smaller segments. These were removed by rolling the resin down an inclined plane, but examination of the spheres collected showed some with cracks which subsequently produced further breakage. The 50W X 8 32-35 mesh sample did not have this defect.

The cumene hydroperoxide used was supplied by Hercules Powder Company as a 70% (wt.) solution in cumene. It contained varying quantities of water up to 1½%. It is relatively stable at room temperature for extended periods, no change in 2 months at 122°F being reported;[35] at 194°F, the percent CHP dropped from 70.5% to 69.5% in two days. The thermal decomposition is autocatalytic, the sample being tested at 194°F dropping to 2.9% in 8 days. Evidence of decomposition was observed after 5 months with the last of a 5 gallon batch kept at room temperature in that an exothermic reaction and a pink color developed on mixing the feeds for 4 runs; normally, they were water-white and no heat effects were observed. The peroxide content of the stock had not dropped appreciably, however, and no abnormal behavior occurred during the 4 runs.

Technical grade acetone was used as the solvent for the quantitative work. Some initial work using cumene as solvent was done which showed it to be unsuitable for this reaction and catalyst system.

EXPERIMENTAL PROCEDURE

An experimental run was begun by bringing the water tank to the desired temperature, setting the stroke length on the feed pump, and mixing sufficient feed of the desired composition. A sample calculation of feed preparation and experimental measurements is given in Appendix C. The feeds were prepared by mixing the calculated quantities of water, acetone, and CHP stock (70% CHP in cumene) in a single container and shaking vigorously to give a homogeneous solution.

Water circulation through the deaerator jacket was begun and the feed pump started. When the liquid level in the feed line fell below the constriction, the feed tank was filled and then stoppered, except for a small vent, to prevent evaporation. Checks on the CHP concentration of the feed in the full and almost empty feed tank showed no change in composition during the time of a run. The pinchcock on the reactor outlet was set to give 5-8 psi on the pressure gauge. After any air bubbles in the reactor had dissolved the water circulation to the reactor jacket was begun. A sample of about 300 cc of feed was required to flush out the system once, after which any adjustment necessary in the water tank temperature to give the desired bed temperature was made.

The exothermic nature of the reaction raised the temperature of the particles and the liquid above the jacket temperature. Evidence is presented subsequently to show that the rise within the particle as referred to the particle surface temperature does not affect the reaction rate. The bulk temperature of the bed, however, does rise measurably

above the jacket temperature, due to the reduced surface area per reaction volume and the use of glass as the material of construction, and this rise can affect the rate of reaction. The use of glass beads to dilute the catalyst bed, as mentioned in the section on equipment, helps control this temperature rise by reducing the heat generated per unit length of the reactor. The jacket temperature was adjusted to bring the bed temperature, as indicated by the axial thermocouple, to within 0.5°C of the desired temperature. For most of the runs the bed temperature was no more than 1°C above the jacket temperature; a uniform axial temperature after about the first half inch of the bed resulted under such conditions, and this was taken as the reaction temperature. For a few runs the reaction rate was high enough to be auto-accelerating, and the temperature rose continuously along the bed until the rate fell due to the drop in CHP concentration.

The approach to steady state was observed by titrating the product for CHP content at 30-45 minute intervals. Product samples were taken by collecting the total output of the system for a short period. To prevent loss by evaporation, the sample bottles were corked and cooled in an ice bath during collection. The flow rate was measured during steady state by collecting a measured volume of the total output for 1.0-1.5 minutes. The variation in the measured rate was observed to be less than 1.0%. Feed samples were also taken during the run; both feed and steady state product samples were analyzed immediately for CHP and then stored at 0°F for further analysis. The run was finished by flushing the system with acetone.

The length of the non-steady state period appeared to be due to the flushing required. Redistribution of water between phases, as indicated by changes in bed volume, was slower than chemical rate equilibrium, as indicated by the development of a steady temperature gradient between the bed and the jacket, but both were more rapid than the observed steady state in the product. A period of $1\frac{1}{2}$ to 4 hours was required to reach steady state; the higher the flow rate, the shorter the time required.

Analytical Methods

The analytical method for determining the concentration of CHP in a sample was essentially that of Kokatnur and Jelling[36] and Siggia.[37] A sample of known volume containing 0.070-0.075 grams of CHP (about 1 cc for 10% (wt.) CHP) was transferred from the sample bottle at 0°C to a refluxing flask with a syringe, care being taken to cool the syringe by flushing several times with the cold sample. Acetone interferes with the analysis; it was removed by evaporating it with an air stream. No CHP was lost using this technique; identical samples, warmed at 25°C and 35°C for both 8 and 15 minutes while being dried with air, gave the same analysis for CHP. 25 milliliters of isopropyl alcohol, $1\frac{1}{4}$ cc glacial acetic acid, and $1\frac{1}{4}$ cc of saturated aqueous potassium iodide were added to the flask; the solution was brought to boiling, refluxed for 3 minutes, and titrated hot with standard 1/10 N. sodium thiosulfate to the disappearance of the free iodine produced from the CHP-iodide reaction. The reactions involved are

$$CHP \longrightarrow [O] + \text{residue}$$

$$[O] + 2H^+ + 2I^- \longrightarrow I_2 + H_2O$$

$$I_2\,(\text{red}) + 2\,Na_2S_2O_3 \longrightarrow 2\,NaI\,(\text{colorless}) + Na_2S_4O_6$$

2 moles of sodium thiosulfate are equivalent to 1 mole of CHP. The concentration of CHP (C_c), moles CHP/cm.^{3}, is calculated from

$$C_c = \frac{(V \text{ ml.} \times 0.1000 \text{ N}) \text{ m. eq. } Na_2S_2O_3}{v \text{ cc (sample volume)}} \times \frac{1 \text{ mole CHP}}{2000 \text{ milliequivalents } Na_2S_2O_3}$$

Direct weighing of the sample to be titrated was a less accurate method due to evaporation of the acetone. The accuracy of the method was checked only by analyzing the stock solution and diluted samples of it. The analyses were consistent with the calculated concentrations. The precision of the method was good, duplicate analyses on a given sample agreeing within a range of 6 parts per thousand. The ratio of input to output concentration was the number of interest, so errors in the accuracy of the two analyses would be expected to cancel out. Because the ratio was close to one for most runs, the error in the term ln (C_{ci}/C_{cf}) due to the random variation in measuring the concentration was estimated to be about 4%.

The phenol analysis was a colorimetric method developed by Lykken et al.[38] The phenol was extracted from the sample by dissolving the latter in 50 cc of cumene and shaking the solution with 10 cc KOH (10%), 5 cc KOH (10%), and 5 cc water for 5, 5, and 2 minutes respectively. Extraction from the CHP was necessary to prevent additional phenol from being formed in subsequent treatment. The aqueous layers were removed from the bottles with syringes, combined in a 100 ml. volumetric flask, and diluted to the mark with glacial acetic acid while cooling in an ice bath. A 1-5 cc aliquot of this solution was transferred to a 50 ml.

volumetric flask. The size of the original sample and the size of the aliquot were controlled to give a final amount of phenol in the range 0.1-0.4 mg. as follows:

wt.% phenol expected	sample size, cc	aliquot cc
0.5	1.0	5.0
1.0	1.0	3.0
2.0	0.5	3.0
4.0	0.5	1.0
8.0	0.5	1.0
10.0	0.3	1.0

The volume of liquid in the 50 ml. flask was made up to 5 cc if necessary with a buffer solution of 15 cc 10% KOH, 5 cc water, and 80 cc glacial acetic acid, and the phenol was converted to p-nitrosophenol by the addition of 2 drops saturated aqueous sodium nitrite and 6 drops concentrated sulfuric acid. The reaction was given 40 minutes at room temperature and the color was developed by slowly adding a solution of isopropyl alcohol-concentrated ammonium hydroxide-water (4.5-3.0-2.5) while cooling in an ice bath. The reactions as suggested by Lykken are

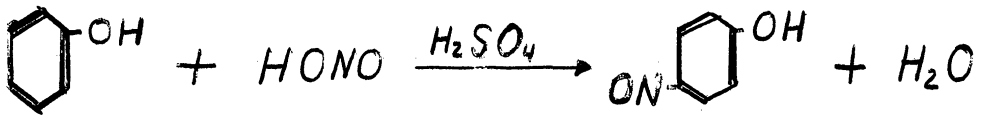

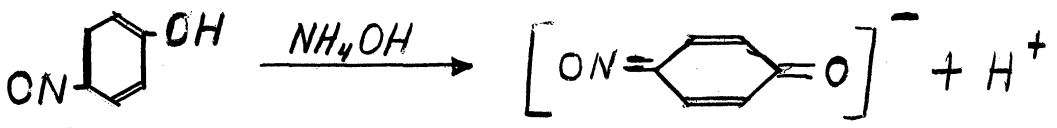

The complex has a characteristic yellow color.

The volume was brought to 50 ml. at room temperature with the ammonia solution and the flask allowed to stand overnight. The % transmission as compared to the IPA-NH_4OH-H_2O solution was measured with a Beckman Model DU Spectrophotometer at 420 microns and a slit width of 0.1 mm. The weight of phenol per 50 ml. of solution was determined from a calibration curve of % transmission versus g mg. phenol per 50 ml. of solution prepared using the above technique and samples of known phenol content. The concentration of phenol C_p, moles phenol/cm.^{3}, in the original sample was calculated from

$$C_p = \frac{\text{g mg. phenol}}{\text{1000 mg./gm.}} \times \frac{\text{100 cc.}}{\text{v' cc aliquot}} \times \frac{\text{1 mol.}}{\text{94.1 gm. phenol}} \times \frac{1}{\text{v cc sample}}$$

The water analysis used was the modified Karl Fisher technique of Peters and Jungnickel,[39] developed to prevent acetone interference, plus corrections from Mitchell and Smith[40] to prevent CHP interference. The procedure consists of titrating a solution of the unknown in an alcoholic solvent with a reagent containing sulfur dioxide and iodine. The reagent was prepared from 450 ml. pyridine, 450 ml. methyl Cellosolve, 133 grams iodine, and 70 ml. liquid SO_2, and stored in an enclosed automatic burette. The reagent degenerates, so it must be standardized daily by titrating a standard H_2O-solvent mixture before use. The solvent is 4:1 ethylene glycol-methyl Cellosolve. The unknown (1 cc for 4-8% (wt.) water) was dissolved in 25 cc of the solvent in a 100 ml. volumetric flask. If a large quantity of CHP was present, it was neutralized with a solution of SO_2 in pyridine. For 10% (wt.) CHP or less, the excess SO_2 in the reagent

provided neutralization without producing undesirable side effects. The unknown in solution was cooled in an ice bath and titrated to the characteristic red-orange end point of free iodine. The basic reaction is:

$$C_5H_5N \cdot I_2 + C_5H_5N \cdot SO_2 + C_5H_5N + H_2O \longrightarrow$$

$$2\,C_5H_5N\langle \begin{matrix} H \\ I \end{matrix} + C_5H_5N\langle \begin{matrix} SO_2 \\ O \end{matrix} \xrightarrow{ROH} C_5H_5N\langle \begin{matrix} H \\ SO_4R \end{matrix}$$

The complete chemistry of the reagent is complex and still in doubt. The visual end point in the volumetric flask was used in preference to an electrometric endpoint because of interference from moisture in the air with the latter. Measurement to 0.1% water was sufficient for the purposes of this study, so that high precision was not required. The volume of reagent required by the unknown and solvent was corrected by that required by the solvent alone and the concentration of water C_w, mol. water/cm.^{3}, calculated from

$$C_w = \frac{V \text{ cc. reagent}}{v \text{ cc. sample}} \times \text{titer of reagent } \left(\frac{\text{mg. water}}{\text{cc. reagent}}\right) \times \frac{1 \text{ mole water}}{18{,}000 \text{ mg. water}}$$

EXPERIMENTAL RESULTS

The experimental data and calculations are reviewed in this section and tabulated in Appendix A. The section following contains a more complete discussion of the effects encountered. The levels of variables studied were: flow rate 0.84 to 5.9 grams/minute (1.4 to 10.0 gm. per (min.)(cm.^{2})); temperature 30, 40, and 50°C; water content 0.4 to 8.4 wt. % (0.2 x 10^{-3} to 4.2 x 10^{-3} moles water/cm.^{3}); CHP content 10, 20, and 30 wt. % (5.5 x 10^{-4}, 11 x 10^{-4}, and 17 x 10^{-4} moles CHP/cm.^{3}); and particle size 32-35 (large), 60-65 (medium), and 115-150 (small) mesh. The solvent for all work was acetone (50-80 wt. %) except as specifically noted in the section on the use of cumene as solvent.

These ranges were found adequate to demonstrate the effects of each variable on the reaction rate. For one run, nominally at room temperature, the high reaction rate resulted in a bed temperature of 70-75°C. The liquid within the bed boiled and the catalyst darkened noticeably under these conditions, indicating the difficulty in operating at high reaction rates and higher temperatures.

Since an integrated correlation approach was used, it was desirable to measure point rates as nearly as possible, that is, to keep the conversion as low as possible consistent with a reasonable accuracy of measurement. The precision of the CHP analysis was good enough to permit an accurate ($\pm$ 3%) determination of the experimental variable k (defined Equation (33) page 29) at conversions of 10%; most runs were made in the range of 10-20% conversion.

Effect of Flow Rate

An increase in the linear velocity of the fluid past the catalyst particles is expected to decrease the mass transfer resistance between the bulk of the liquid and the liquid-solid interface. The transfer of CHP into the particles will result in a concentration gradient, but if the flow rate is high enough the difference between the bulk concentration and the surface concentration should be negligible.

Theoretically, the effect is most easily studied at a maximum reaction rate, since this would result in the highest concentration gradient across the liquid film; an increase in flow rate under these conditions would have a more significant effect on the surface concentration of CHP and therefore on the rate. Experimentally, the high heat release associated with the high reaction rate interferred with precise measurements. For the run the catalyst bed was divided into five parts, four 1/4 inch long, one 5/8 inch long, separated by glass beads and glass wool. This permitted the reciprocal space velocity N/W (and thus the conversion) to be held approximately constant by removing a section each time the flow rate was lowered, thus assuring that only the effect of flow rate and not the method of rate estimation was being tested.

The data for the run are listed in Table I. The small Dowex 50 X 8 resin was used, at (nominal) 50°C, 2% water, and 10% CHP, with a difference from inlet to outlet of about 1.5% CHP. The temperature rose to a maximum of 51.2°C in the large (fifth) bed section at W = 4.66 gm./min., giving a high k, since dk/dT is approximately 12 gm. per(min)(equiv. H^+)(°C) for this reaction rate. For the other flow rates, the shorter bed

TABLE I

Effect of Flow Rate on the k Value at a High Reaction Rate.

Data of Run 30: 50°C (nominal), 2% water, 10% CHP, 3.3% cumene, and 84.7% acetone.

W Flow Rate gm./min.	$\frac{N}{W}$ $\frac{(\text{equiv. } H^+)(\text{min.})}{\text{gram}}$	$\ln \frac{C_{ci}}{C_{cf}}$	k $\frac{\text{gram}}{(\text{min.})(\text{equiv.} H^+)}$
4.66	.001342	.176	131.1
3.12	.001204	.146	121.1
2.06	.001368	.174	126.9
1.52	.001242	.162	130.2

lengths permitted better cooling, and the temperature indicated by the axial thermocouple held at 50.5°C. Due to the short bed lengths and the resultant end effects, the temperature indicated was probably below the actual reaction temperature. As the flow rate was decreased, greater quantities of heat were released per unit length, giving a gradual rise in average reaction temperature and k. Any flow effect is thus masked by the temperature effect, which shows a variation of $\pm$ 3%.

Data were taken at a lower reaction rate to eliminate the effect of temperature rise (Table II). The bed size was constant for the series, so an increase in conversion resulted as the flow rate was reduced. The k's are thus measured at different average CHP concentrations but at a constant water content. As is discussed later, this results in a variation in k; at a given water content, the higher the CHP content, the lower the k value measured. This can be seen by referring to Figure 10, page 59. The four values of k from Table II are plotted in this figure at $C_W = 3.0 \times 10^{-3}$ moles water/cm.^{3}. The decrease in k from 9.40 to 8.76 gm. per (min.) (equiv. H^+) can be accounted for by the increase in C_c (ln mean) from

TABLE II

Effect of Flow Rate on the k Value at a Low Reaction Rate.

Data of Run 12: 50.2°C, 6.3% water, 20% CHP, 6.6% cumene, and 67.1% acetone.

W Flow Rate gm./min.	$10^4 C_c$ (ln mean) moles CHP/cm.^{3}	k $\frac{\text{gram}}{(\text{min.})(\text{equiv.}H^+)}$
1.21	10.6	9.40
2.53	11.2	9.20
3.37	11.5	9.10
5.84	11.6	8.76

10.6×10^{-4} to 11.6×10^{-4} mol. CHP/cm.^{3} and therefore no effect of k was found in changing W by a factor of about 5:1. Runs 15 and 17 at 10% CHP gave pairs of k values at two flow rates which when corrected for the effect of change in C_c (ln mean) had a drop of about 4% from the higher to the lower flow rates, $W_{minimum}$ being 0.84 and 1.76 gm./min. It was decided to set $W_{min.}$ at 2.0 gm./min. for subsequent investigation and to assume negligible mass transfer resistance above this value, i.e., Equation (30), page 28, holds.

Precision and Reproducibility of k Value Measurements

Estimates of the precision which can be attributed to the numbers from which k is calculated (N, W, C_{ci}, and C_{cf}) were made on the basis of experimental duplication. The flow rate W was measured by collecting a measured volume of feed over a 1.25-1.50 minute interval.

Periodic measurements during a given run gave flow rates within one part per hundred precision, which is consistent with errors of 0.02 cc. and 0.01 min. in the volume and time measurements.

The value of N was calculated from the weight of resin charged and the capacity of a sample from the same bottle. The latter was determined by titration with standard base. The precision of the titration was measured as 3 parts per 400 for triplicate samples. The 1-2 gram samples of resin were weighed to 0.1 mg. The error in N was thus estimated at less than 1%.

The values of C_{ci} and C_{cf} from duplicate samples agreed within a range of 6 parts per 1000. On this basis the value of $\ln (C_{ci}/C_{cf})$, which was small because C_{ci}/C_{cf} was close to one, was estimated to have an error of 4%. The error in k was therefore estimated to be about 5%, from the combination of these errors. The experimental reproducibility of the k values was somewhat better than this, about 2-3%. The difference is probably due to the error estimate for the log term being too high. Taking duplicate samples and using the same technique for measuring both C_{ci} and C_{cf} gives a better value for the ratio due to cancellation of errors than the precision in a single measurement of C_c would indicate.

Table III gives pairs of k values from repeated runs at three reaction rates. The values vary by 2% from each other. Runs 13 and 24 were made with a single catalyst charge at the beginning and end of its use, while 39-40 and 59-60 are runs with the same feeds and two different catalyst charges.

TABLE III

Reproducibility of k values.

Run	Temp. °C	$10^3 C_w$ moles water / $cm.^3$	Flow Rate W gm./min.	N equiv.H^+ in reactor	k gram / (min.)(equiv.H^+)
13	49.7	3.0	1.72	.0300	11.3
24	50.5	3.0	1.95	.0300	11.2
39	40.5	0.74	2.08	.00524	52.5
59	40.5	0.74	2.09	.00465	51.2
40	50.5	0.74	3.49	.00524	130.0
60	50.5	0.74	3.34	.00465	127.1

Effect of Water Concentration

After much trial and error the water concentration was found to be an important variable in determining the rate. Acetone was chosen as the solvent for the reaction in place of cumene, in which initial work was done, because the system CHP-acetone-water is one phase at the concentrations of interest while CHP-cumene-water is two phases. Also a medium in which the phase distribution of water would reach steady state rapidly was desired; because of the low solubility of water in cumene, steady state was approached very slowly when the water content of the resin phase was above the equilibrium value of a feed made with cumene. Acetone proved satisfactory from this aspect.

Figure 6 shows the relation between the experimental variable k and C_w, the concentration of water in the feed, at 30 and 50°C; these data were obtained with the large 8% cross-linked resin at 10% CHP. Figure 7 gives similar curves obtained with the medium 8% cross-linked resin,

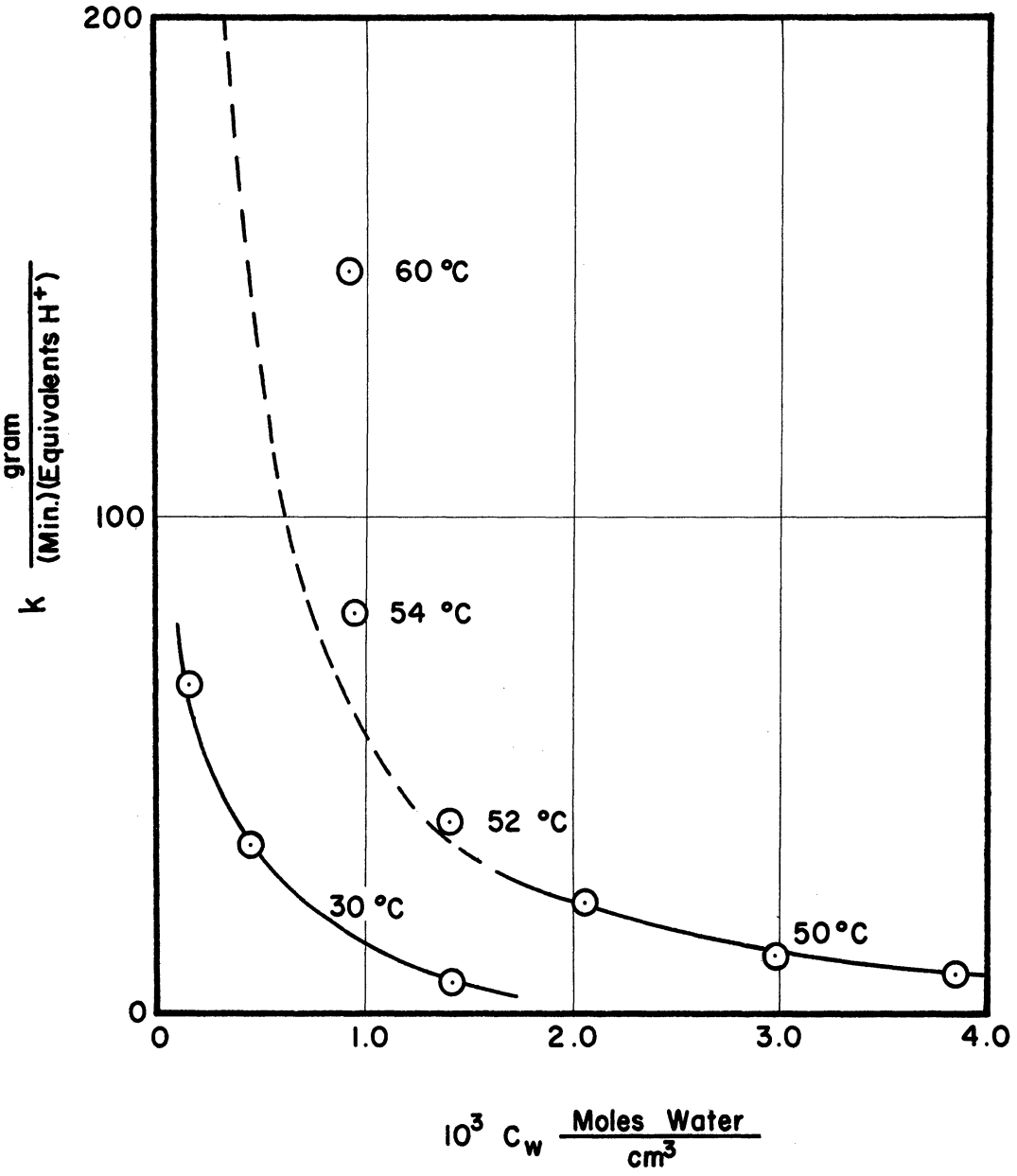

Effect of Water Content on k; 32-35 mesh Dowex 50 X 8, 10% CHP.

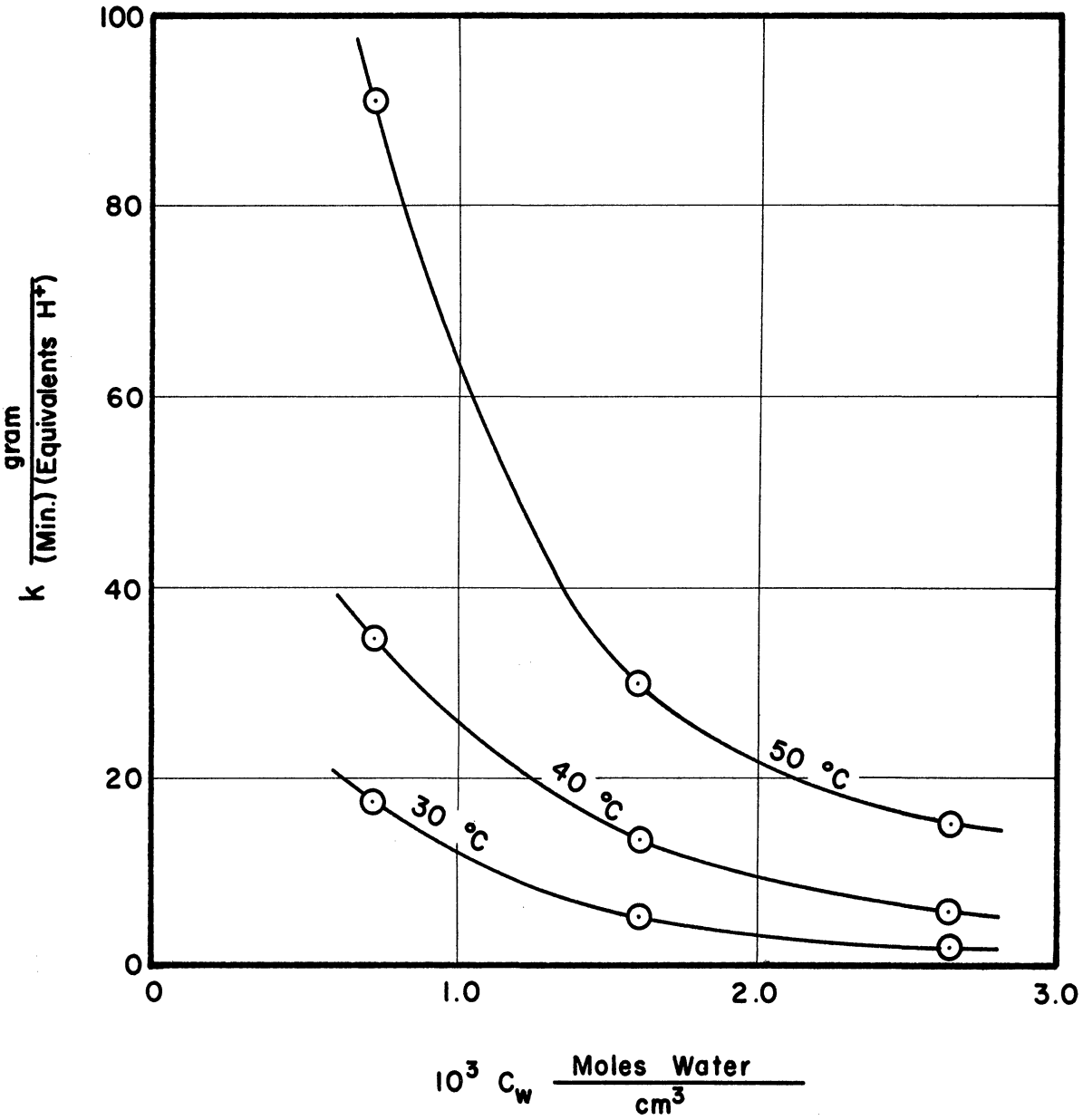

Figure 7. Effect of Water Content on k; 60-65 mesh Dowex 50 X 8, 10% CHP.

again at 10% CHP but at three temperatures. In Figure 6, the location of the 50°C curve at the lower values of C_w(dotted section) has been estimated with respect to the 30°C curve from the points obtained at temperatures slightly above 50°C and from the temperature effects measured with the other particle sizes. The catalyst bed was not diluted with glass beads for these runs, so uniform temperatures (and the desired level) were not maintained at the higher rates of reaction.

Effect of Particle Size and Resin Grade

A series of runs was made using a given batch of feed at a given temperature for all three particle sizes of Dowex 50 X 8 resin. k values for the small size particles were 1.5 times the k values from the medium size particles, while the k values from the medium and large size particles were within 10% of each other. The small-medium pairs would indicate that size is important, while the medium-large pairs indicate that the particle size is not important.

The contradiction was resolved by the observation that the mechanical stability of the 32-35 mesh (large) Dowex 50 X 8 was poor. Cracks in the resin spheres of this size were observable under a microscope before the catalyst had been used, and the stresses incurred by solvent absorption gave further breakage during runs. 32-35 mesh Dowex 50W X 8, a more stable form of the resin made by a different process, gave k values which were about 40% of the k values obtained under corresponding conditions with the medium size particles. For a high value

of α (reaction rate very rapid compared to diffusion rate), the reaction rate per unit volume of catalyst is reduced by a factor of $\frac{1}{2}$ if the particle size is doubled; with a lower ratio of chemical rate to diffusion rate, the reaction rate for the larger particle must be between 50 and 100% of the rate for the smaller particle. The fact that the k value for the Dowex 50W X 8 32-35 mesh (large) resin is 40% of the k value for Dowex 50 X 8 60-65 mesh (medium) resin suggests that the two resin grades are not exactly comparable.

Table IV gives one set of k values for the three 50 X 8 and one 50W X 8 particle sizes, other variables being constant. Since the rate is dependent on particle size, a small particle size will give more efficient catalyst utilization than a large size.

TABLE IV

Effect of Particle Size on k Value: 40°C, 10% CHP, 5.8% water, 3.3% cumene, 80.9% acetone.

Run	Resin type and size	k $\frac{\text{gram}}{(\text{min})(\text{equiv.}H^+)}$	k/6.15
33	50X8 S	9.24	1.50
43	50X8 M	6.15	1.00
52	50X8 L	5.49	0.89
65	50WX8 L	2.69	0.44

Effect of Temperature

The effect of temperature was investigated at three levels of water concentration for all particle sizes. The rate of reaction increased with increasing temperature in an exponential manner as can be seen from

Figures 8 and 9. The data for Figure 8 were measured with the medium resin, while the data for Figure 9 were obtained with the small resin under the same conditions. The temperature control for these data was good, i.e., a uniform temperature was maintained along the bed, with glass beads being used as diluent for high reaction rate measurement. The bed temperature as measured axially midway from the ends of the bed was recorded as the reaction temperature.

Effect of CHP Concentration

The effect on k of varying the CHP concentration is shown in Figure 10, in which the factor % CHP is shown as a parameter for a family of curves of k gm. per (min.)(equiv.H^+) versus C_w moles water/cm.^{3} The pseudo-order of the reaction as a function of C_w can be calculated from this figure. At $C_w = 2.75 \times 10^{-3}$ moles water/cm.^{3}, $C_{c_1} = 5.5 \times 10^{-4}$ moles CHP/cm.^{3}, and $C_{c_2} = 11.0 \times 10^{-4}$ moles CHP/cm.^{3}, the experimental k's are $k_1 = 13.1$ and $k_2 = 9.7$ gm. per (min.) - (equiv.H^+). $R = k(m/\rho)C_c$, with (m/ρ) being estimated as 4.31×10^{-3} equiv. H^+/gram. Thus $R_1 = 13.1 \times 4.31 \times 10^{-3} \times 5.5 \times 10^{-4} = 3.10 \times 10^{-5}$ moles CHP per (min.)(cm.^{3}) and $R_2 = 9.7 \times 4.31 \times 10^{-3} \times 11.0 \times 10^{-4} = 4.60 \times 10^{-5}$ mol. CHP per (min.)(cm.^{3}). Doubling the CHP concentration increases the rate by a factor of 1.5, indicating an order of 0.6. From estimates of $k_1 = 5.0$ and $k_2 = 2.5$ gm. per (min.)(equiv.H^+) at $C_w = 5.5 \times 10^{-3}$ mol. water/cm.^{3}, values of $R_1 = 5.0 \times 4.31 \times 10^{-3} \times 5.5 \times 10^{-4} = 1.19 \times 10^{-5}$ and $R_2 = 2.5 \times 4.31 \times 10^{-3} \times 11.0 \times 10^{-4} = 1.19 \times 10^{-5}$ mol. CHP per (min.)(cm.^{3}) would be predicted. These values would indicate a zero order reaction; changing the CHP concentration has no effect on the reaction rate. The interpretation is not

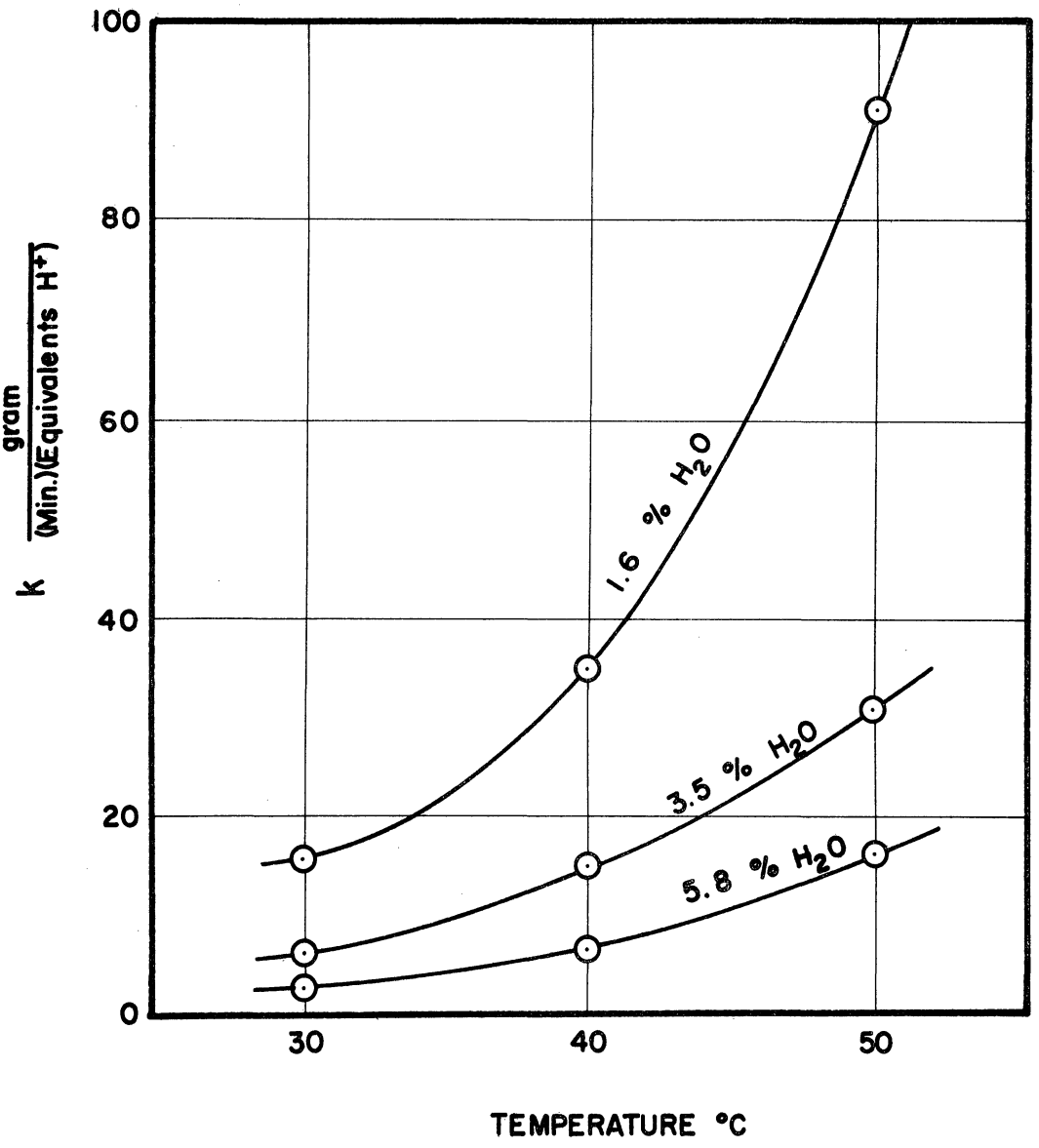

Figure 8. Effect of Temperature on k; 60-65 mesh Dowex 50X 8.

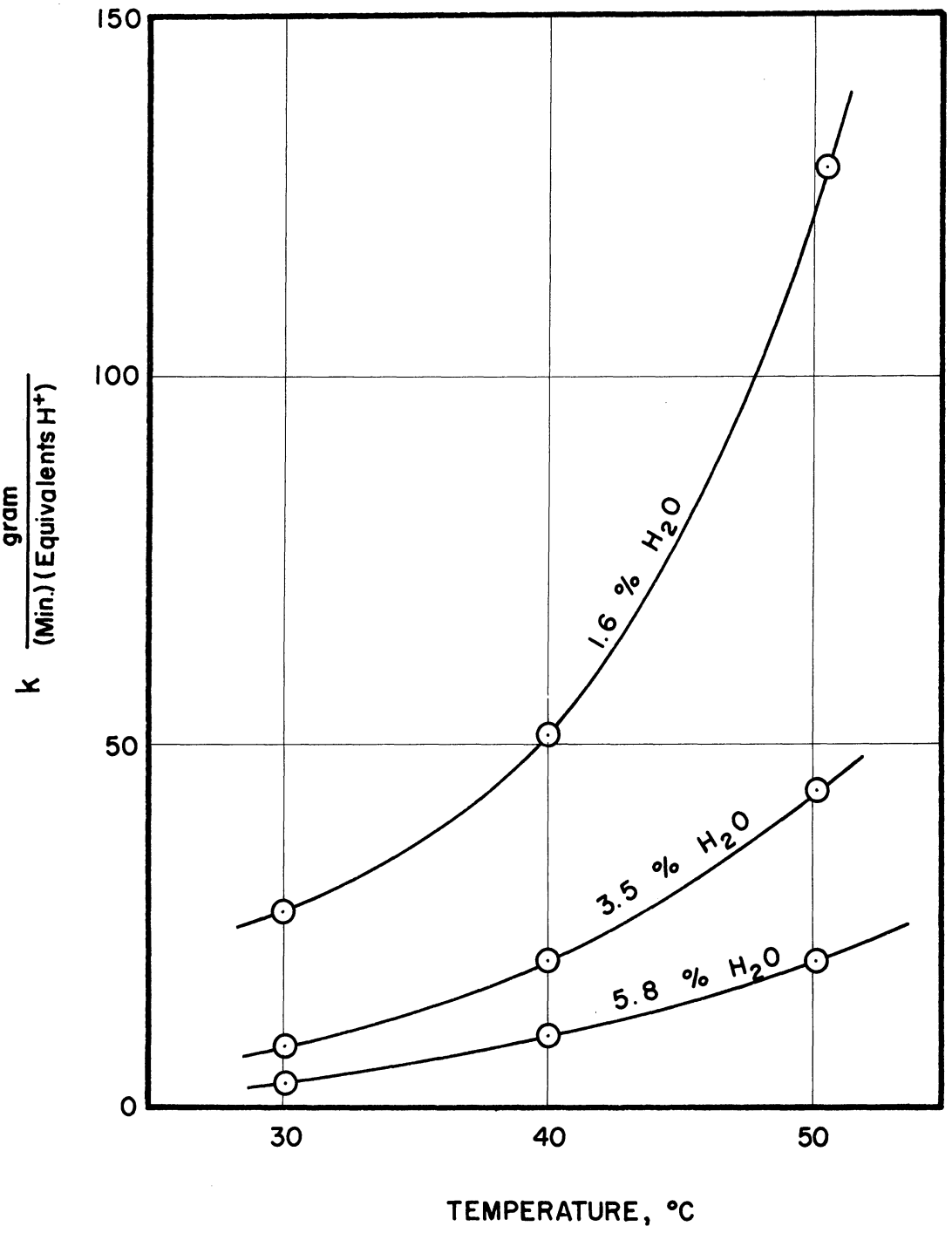

Figure 9. Effect of Temperature on k; 115-150 mesh Dowex 50 X 8.

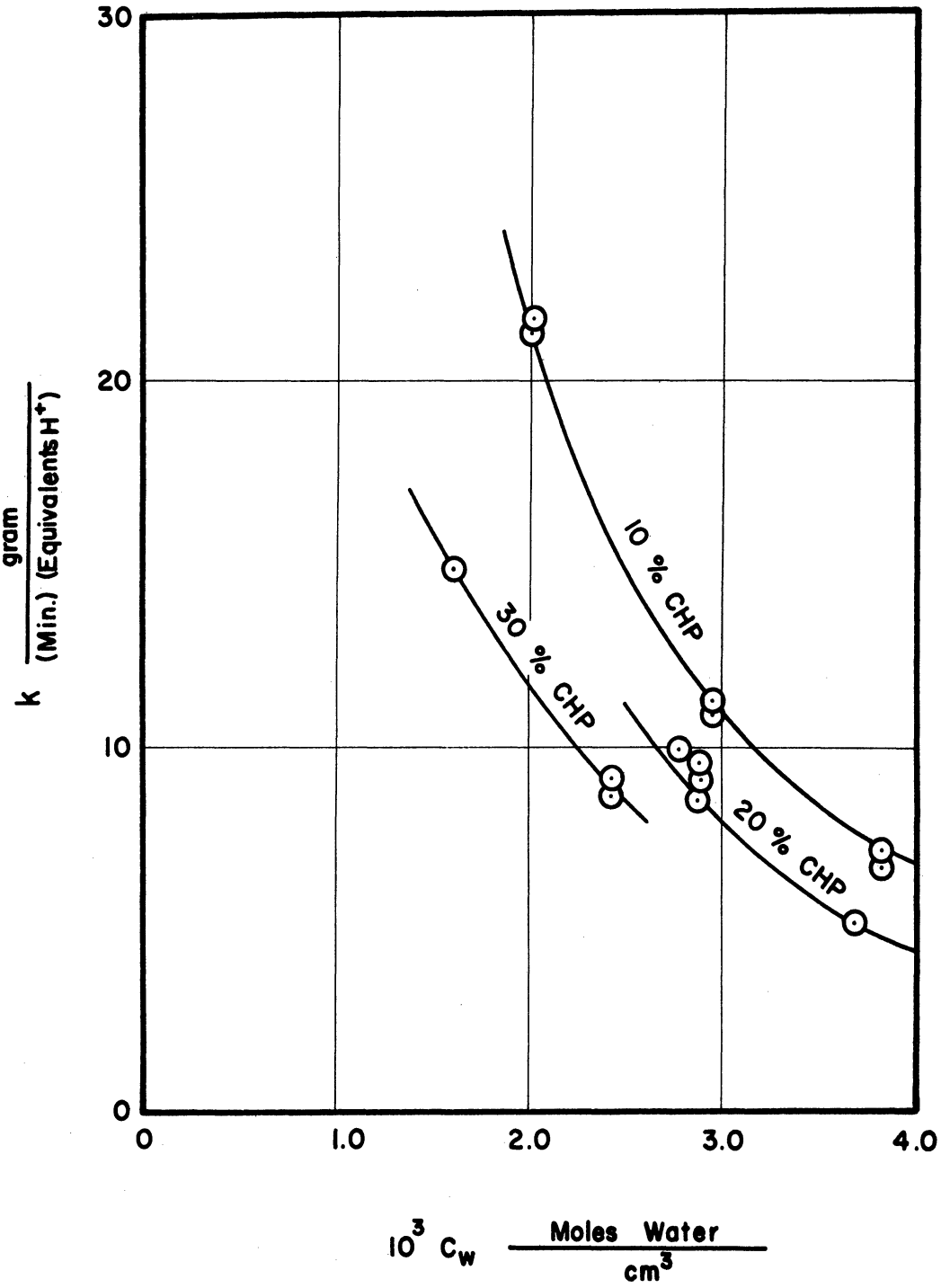

Figure 10: Effect of CHP Concentration on k; 32-35 mesh Dowex 50 X 8, 50°C.

made that the order is a function of water content; the data are explained by phase distribution effects. Increasing the external CHP concentration increases the phase distribution coefficient of water and decreases the phase distribution coefficient of CHP, so that the rate is not doubled by doubling C_c.

The Yield of Phenol

The yield of phenol is calculated from the gain in phenol concentration and the loss of CHP and is expressed as the percent of the theoretical which is actually obtained:

$$\% \text{ yield} = \frac{C_{pf}/\rho_f - C_{pi}/\rho_i}{C_{ci}/\rho_i - C_{cf}/\rho_f} \times 100\%$$

High conversion runs were made to reduce the error in the calculation. The yields obtained were 89.1% for a 2% water feed and 90.5% for a 4% water feed, which is the same as the yield reported for the homogeneous reaction (90%). It was expected that secondary reactions might reduce the yield as the water content was lowered, but at 2% water and 50-60°C the reaction was still specific for phenol.

Analyses for the increase in phenol concentration were made on the feed and product samples of low conversion runs, but because the precision of a single analysis was only $\pm$ 3 parts in 100, little significance could be attached to the values of % yield calculated; they ranged from 70 to 120%. Because of this lack of precision, no attempt was made to study the rate process (i.e., the specificity as a function of reaction conditions) with this analysis.

The products of the high conversion runs were steam distilled in an attempt to recover byproducts for analysis (normal distillation would result in decomposition of the reaction products) but because the total quantity of byproduct was low (1% of the product), no significant fraction was obtained. No conclusions are made concerning the nature of the byproducts.

DISCUSSION

Phase Distribution

The concept of phase distribution is important in interpreting the rate data because all the variables except particles size can be expected to affect the phase distribution coefficient for CHP, i.e., the ratio of resin phase concentration to liquid phase concentration. The true activation energy of the chemical reaction, for example, cannot be measured by the effect of temperature changes on the rate, because the changes may cause phase shifts simultaneously.

The discovery that the rate was inversely proportional to the water concentration resulted from the facts that water is not involved in the stoichiometry of the reaction and that the stock 70% CHP did not have a constant water content from batch to batch. Techniques which gave reaction with one batch gave no reaction with the following batch until water was added. Most work with ion-exchange resins as acid catalysts has involved hydrolysis, hydration, or dehydration,[27,28,30,41,42,43] so that chemical effects from water were expected, and the data were interpreted in terms of significant reverse reactions.

The rate is sensitive to water concentration, in particular, because water has a high phase-distribution coefficient, giving a resin phase which is aqueous although the liquid phase may contain only a small percent of water. Davies and Owen[23] measured the distribution of water and acetone in the two-phase system. With 3 wt. % water in the liquid phase, the resin phase of 5.5% divinylbenzene resin was 49% water, while

10% divinylbenzene resin contained a liquid of 62% water. CHP is not soluble in water, but it does dissolve in a water-acetone mixture; the higher the proportion of water to acetone, the lower the solubility of CHP. The inverse effect of water on the rate of reaction at a constant CHP level is interpreted as resulting from a shift in the solubility of CHP in the resin phase as the proportion of water to acetone changes. Likewise, an increase in CHP content (externally) must be done at the expense of the acetone fraction; the CHP in the resin phase increases less than proportionally, and the measured rate does not show a first order relation.

Water is of course just one possible component; more generally, the value of λ will be a function of the total external phase composition as well as the cross-linking of the resin. Alcohols, for instance, also have high phase-distribution coefficients; since they should be more compatible with CHP their use as solvents might be of interest for future work.

Two k values were measured with a lower cross-linked resin (60-65 mesh 4% divinylbenzene). They were appreciably higher than the k values from 60-65 mesh 8% divinylbenzene resin at the same conditions: at 40°C, 5.5% water, and 10% CHP the values were (4% DVB) 8.97 gm. per (min.)(equiv.H^+) versus (8% DVB) 6.15 gm. per (min.)(equiv.H^+); at 50°C, 5.8% water, and 10% CHP they were (4% DVB) 25.6 gm. per (min.)(equiv.H^+) and (8% DVB) 14.5 gm. per (min.)(equiv.H^+). The effect of an increase in cross-linking on water-acetone distribution which would predict a lower rate has been noted, and there may also have been a reduced resistance to diffusion in the more open network occurring simultaneously which would give a higher rate.

Behavior of the Catalyst

The size of a catalyst particle changes with changes in the external environment. The volume of 60-65 mesh Dowex 50 X 8 varies in the ratios 1.0-1.6-2.1 under cumene, acetone, and water respectively, with the volume under cumene about the same as the air dry volume. The percent increase in volume is independent of resin size, so that the three sizes studied in this work maintained the diameter ratios of 4:2:1 in changing environments. The diameter in equilibrium with a multicomponent mixture is a function of composition and temperature.

Each sample of resin used has a range of particle sizes between the two mesh sizes; the size distribution within this range is assumed to be uniform, and the sample is characterized by the arithmetical average of the extremes, since the range of sizes is narrow. This average value was estimated to change by $\pm 2\frac{1}{2}\%$ from observations on the total bed volume. The diameters in centimeters under different conditions are

mesh size	air dry size range, cm.	avg. diam. air dry, cm.	range of diam. under reaction conditions, cm.
32-35	.0417-.0495	0.0456	.0540-.0566
60-65	.0208-.0246	0.0227	.0270-.0283
115-150	.0104-.0124	0.0114	.0135-.0142

The upper limits of the size under reaction conditions apply to the conditions of highest water content and lowest temperature, and vice versa.

Changes in the total bed volume were observable in the glass reactor. Normal operation consisted in making the runs with a given catalyst charge in such an order that the particle and total bed size decreased from one run to the next, allowing the bed to remain in a loosely settled

form. Expansion in the bed was restricted; when large expansions were necessary, back flow was used to suspend the particles to allow them to resettle in a loose bed.

Water had a chemical effect as well as the physical effect noted previously. Two regions of different chemical behavior were investigated, the boundary between the regions being a function of temperature and water content. For high water contents, the catalyst remained a light yellow-orange, while at reduced water content the catalyst darkened continuously until becoming black. The total acidity of a catalyst batch was constant in both regions but the specific acidity of the darkened catalyst was decreased, apparently due to the increased weight from the dark substances. If the conditions for darkening were not prolonged the color which had developed could be removed by a high (greater than 2%) water content feed. Completely darkened catalyst lost some colored material to a high water content feed without becoming noticeably lighter, indicating that it was not a completely reversible phenomenon.

The cause of the darkening is considered to be the increased rate of secondary reactions. Thermal decomposition of phenol is enhanced by the absence of water; steam distillation of phenol is used to purify it, while in a normal distillation of a phenol-water mixture discoloration begins as the water is distilled off but before a large temperature rise occurs. The condensation of acetone with itself requires a low water content,[42] and the catalyst is darkened during that reaction. From the mechanism suggested by Seubold and Vaughan (page 5) it can be seen that changes in water concentration could affect the rate at two steps. If

the reverse rates of the sequence are negligible, the step involving addition of water to the rearranged intermediate would be the critical point; lowering the water concentration could result in a reaction occurring more readily between the carbonium ion and some other component of the system, including the resin.

If the decomposition and secondary reaction products are bulky or attach themselves to the resin, they will not be able to diffuse out of the resin network from the internal sites where they are formed. The darkening of the catalyst is attributed to the buildup of these substances, the phenol decomposition products in particular being noted for being colored.

The anhydrous region of operation would thus not be suitable for commercial operation; the loss of phenol to byproducts would offset the increased rate. No sustained operation in the anhydrous region was made, but it might be comparable to operation with cumene as the solvent, which is discussed later. The buildup of compounds blocking the network would be expected to prevent diffusion of CHP into the resin and thus to destroy the catalyst's effectiveness eventually.

The secondary reactions become important below 2% water for 10% CHP; as mentioned previously, the phenol yield at 2% water was not significantly different from that at 4% water. k values were measured at 1.6% water with no darkening during the run, but the catalyst then turned dark on standing overnight, even with washing. The boundary between the two regions of high yield and high secondary reactions is therefore at about

1.5% water for 10% CHP and 50°C. The darkening appeared to be a function of temperature; the high rate resulting from the minimum water content run produced non-uniform temperatures along the bed, and the initial (and cooler) portion of the bed darkened more slowly than the final part. A buildup of byproducts in the feed stream may have also contributed, of course.

The lifetime of the catalyst in a steady state system is of interest. Catalyst degradation was studied by two methods, reproducibility of results and titration of the acidity of the total charge after use. The longest period of use for one batch of catalyst was 165 hours reaction time over a 30 day period. Run 13, the third run, and Run 24, the next to last run of the series, gave k values within 2.1% for the same conditions, indicating no degradation. This series included a few runs of 2% water or less, which is the boundary between the stable and non-stable regions. The titration method was used on charges with less reaction time, again with no degradation noticed. The total acidity checked within $1\frac{1}{2}$% of the calculated charged acidity. Except for the large Dowex 50 X 8, which was susceptible to breakage as has been noted, the catalyst maintained its spherical form and remained free flowing when reaction conditions were kept in the region of stable operation.

Comparison with Homogeneous Rate

Seubold and Vaughan[5] correlated their data of the decomposition of CHP by strong acid in homogeneous solution by the equation

$$-\frac{d[CHP]}{d\theta} = k_2[H_3O^+][CHP] \quad \frac{\text{mol. CHP}}{(\text{sec.})(\text{kg.})}$$

where the concentrations are moles per kg. and k_2 has the units kg. per (mol. H_3O^+)(sec.). This can be expressed as a rate R mol. CHP per (min.) (cm.^{3}) by multiplying by ρ gm./cm.^{3}, 1 kg./1000 gm., and 60 sec./min.

$$R = -\frac{60\,\rho}{1000}\frac{d[CHP]}{d\theta} = \frac{60\,\rho\,k_2}{1000}[H_3O^+][CHP]$$

The data from this study are correlated by the equation

$$R = k(m/\rho)\,C_c$$

where k is in gm. per (min.)(equiv.H^+), C_c is mol. CHP/cm.^{3}, and (m/ρ) is equiv.H^+/gm. Setting the two rates equal permits derivation of the relationship between k_2 and k:

$$k(m/\rho)\,C_c = \frac{60\,\rho\,k_2}{1000}[H_3O^+][CHP]$$

Since

$$C_c = \frac{\rho[CHP]}{1000} \quad \frac{\text{mol. CHP}}{\text{cm.}^3}$$

and

$$1000(m/\rho) \times \frac{1\text{ mol } H_3O^+}{1\text{ equiv. } H^+} = [H_3O^+]$$

then

$$k = 6.0 \times 10^4\, k_2$$

At 50°C, Seubold and Vaughan report k_2 = 0.00101 kg. per (mol.H_3O^+)(sec.) from which the corresponding k value is calculated to be 60.6 gm. per (min.)(equiv.H^+). Figure 9, page 58, gives k values at 50°C as a function

of water concentration for the small resin ranging from 25 to 130 gm. per (min.)(equiv.H^+). The data are thus of the same order of magnitude. Since k values higher than 60.6 were measured with the resin at 50°C, the homogeneous rate might be increased by using a water concentration below that used by Seubold and Vaughan, whose solvent was 50 wt. % acetic acid.

The Use of Cumene as Solvent

Considerable initial work was done using cumene as the solvent for the system. It can be characterized as producing inconsistent and non-reproducible results, the difficulty resulting from a lack of knowledge of the factors involved, primarily the effect of traces of water and changes in the catalyst due to the reaction.

The solubility of water in the cumene-CHP system is low but is increased by increasing the CHP content. One batch of stock CHP contained very little water, so that feeds as low as 0.44% water at 20% CHP could be made. The effect of adding water to a 20% CHP feed in cumene from this stock, shown in Figure 11, is opposite to that found in acetone; increasing the water content increased the rate, with a minimum quantity of water required before any reaction occurred. Two processes may be occurring to promote the rate as water is added: expansion of the resin network by water absorption until the network is opened enough to permit CHP to diffuse in and a shift of environment in favor of the acid-catalyzed ionic reaction.

The order of the runs for this series is important; each succeeding run had a higher water content. Attempts to reproduce the rates

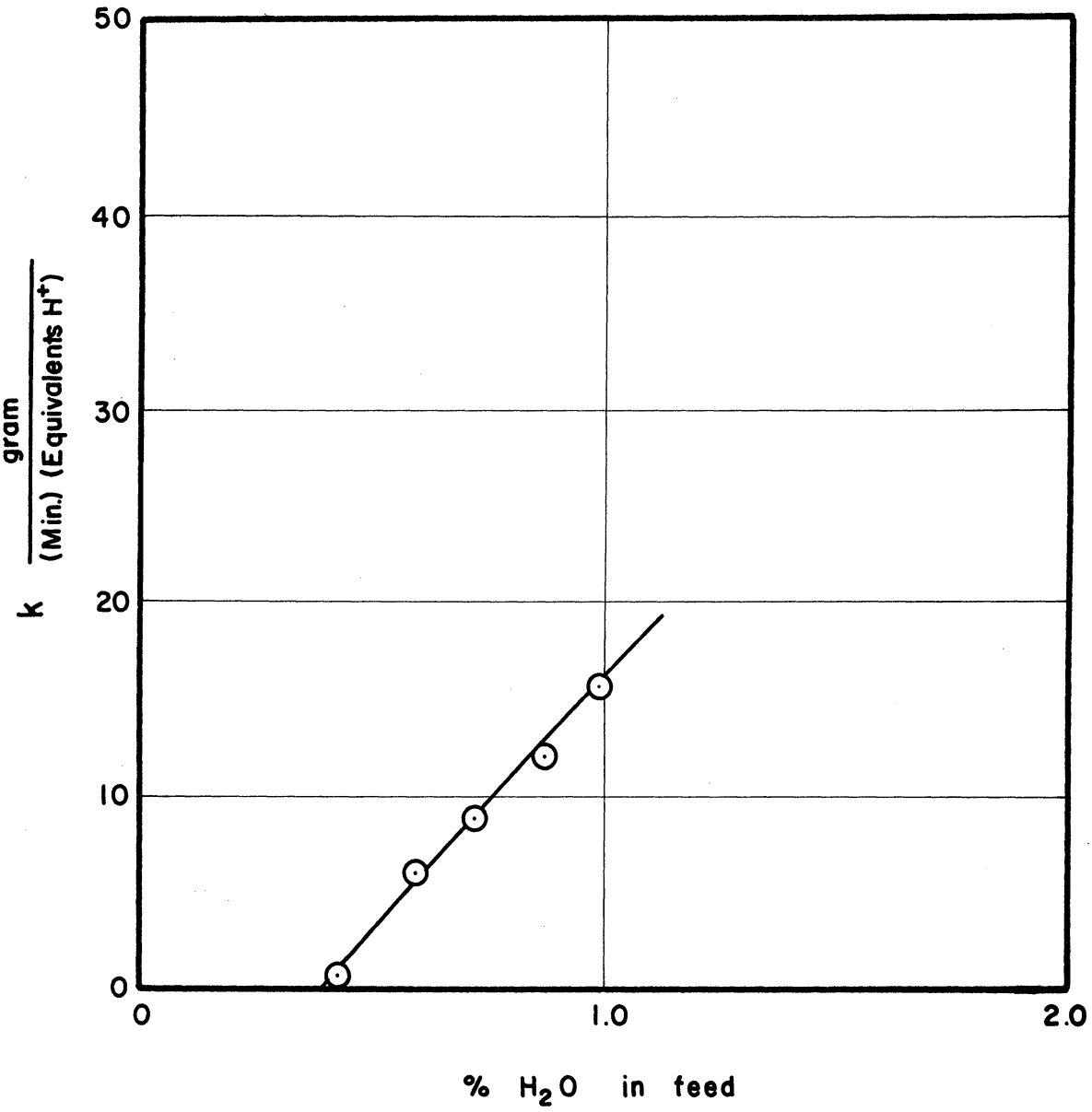

Figure 11. Effect of Water on k using Cumene as Solvent. 115-150 mesh Dowex 50 X 8, 50°C, 20% CHP.

at less than 1% water gave non-steady k values; the rates started at a level corresponding to k = 15 gm. per (min.)(equiv.) and gradually dropped, without reaching the value previously obtained at the same water concentration. The feed had a low capacity for desorbing water from the resin, so the rates were maintained above the values obtained starting with a dry feed and dry resin by the water absorbed in the resin in the preceeding runs.

A few runs were made in which the product of one was collected and used as the feed for the next, giving data equivalent to that from sampling at intermediate points along a long bed. The rates frequently increased from the initial rate, then dropped off. The products of the reaction created an environment which promoted the rate, giving a peak in the rate curve as a function of CHP concentration.

The catalyst turned dark very quickly using cumene as solvent. Phenol yield measurements on the low conversion runs did not have high accuracy, but the measured yields went from 55% to 100%, as compared to the 70-120% range recorded using acetone as solvent. Again, byproducts from reactions other then the primary one are suggested as the cause of darkening, the reaction being considered less specific as a result of the nonpolar solvent. With sustained use the catalyst gradually cracked into fine pieces and froze into place, having to be chipped out of the reactor when changed. The cracked, used resin gave higher rates than the fresh, probably due to the increased surface area.

CORRELATION

The model for correlation derived in the theory section states that

$$k = \frac{k_1 \phi \lambda \rho}{m} = \frac{W}{N} \ln \frac{C_{ci}}{C_{cf}} \qquad (33)$$

where k is an experimental variable, gm. per (min.)(equiv.H^+); k_1 is the rate constant for the homogeneous reaction, min.$^{-1}$; ρ/m is in gram/equiv.H^+; ϕ is a dimensionless function of particle radius r, cm., and the parameter $\alpha = (k_1/D)^{\frac{1}{2}}$ cm.$^{-1}$, where D is the diffusivity of CHP, cm.^{2}/min.; and λ is the phase distribution coefficient for CHP, resin phase concentration/liquid phase concentration. The variation in k with the parameters temperature T°C, particle radius r cm., and liquid phase compositions C_j was correlated on the basis that $k_1 = f(T)$, $\phi = f(r)$, and $\lambda = f(C_j)$, with ρ/m being assumed constant. The form of the function for $k_1 = f(T)$ was taken to be the Arrhenius function, that is, $k_1 = A\, e^{-E/RT}$; the form for $\phi = f(r)$ was derived in the theory section (Equation 25); and no theoretical form was known for $\lambda = f(C_j)$, so an empirical approach was taken in determining the correlation.

The data for a given composition were obtained using a single batch of feed mixed in sufficient quantity to make runs with each particle size at each temperature. This ensured constant water content. Small corrections were applied as needed to bring the k values (measured at, say, 40.0 ± 0.5°C) to a common temperature basis. The resulting values of k are given in Table V for small and medium particle sizes at each temperature-water concentration level.

TABLE V

Values of k for Correlation. From small ($k_{(S)}$) and medium ($k_{(M)}$) particles, with corresponding values of ϕ ratio and α.

$10^3 C_w$	Temp.	$k_{(S)}$	$k_{(M)}$	ϕ ratio	α
mol.water / cc.	°C	gram / (min.)(equiv.H^+)			cm.$^{-1}$
2.7	50.0	19.52	14.30	1.36	125
	40.0	9.24	6.15	1.50	168
	30.0	2.90	2.07	1.40	136
1.6	50.0	43.0	28.5	1.51	172
	40.0	19.42	12.80	1.52	175
	30.0	7.05	5.40	1.30	109
0.74	50.0	124.0	89.2	1.39	132
	40.0	50.2	33.5	1.50	168
	30.0	25.8	16.4	1.57	196

The relation defining ϕ is

$$\phi = 3\left(\frac{\alpha r \cosh(\alpha r) - \sinh(\alpha r)}{\alpha^2 r^2 \sinh(\alpha r)}\right) \qquad (25)$$

where r is the particle radius, cm., and $\alpha = (k_1/D)^{\frac{1}{2}}$ cm.$^{-1}$ The ratio of k's determined with the small (S) and medium (M) particles for other conditions constant equals the ratio of the two values of ϕ, since ϕ is the only factor which is a function of r:

$$\frac{k_{(S)}}{k_{(M)}} = \frac{k_1(\rho/m)\phi_{(S)}\lambda}{k_1(\rho/m)\phi_{(M)}\lambda} = \frac{\phi_{(S)}}{\phi_{(M)}} = \phi_{ratio} \qquad (34)$$

With $r_{(S)}$ = 0.0138 cm. and $r_{(M)}$ = 0.0276 cm. given, ϕ ratio is a function of α only. Figure 12 shows the relationship. Since $r_{(M)} = 2r_{(S)}$, the value of ϕ ratio goes to 1.0 as $\alpha \to 0$ and approaches 2.0 as $\alpha \to \infty$.

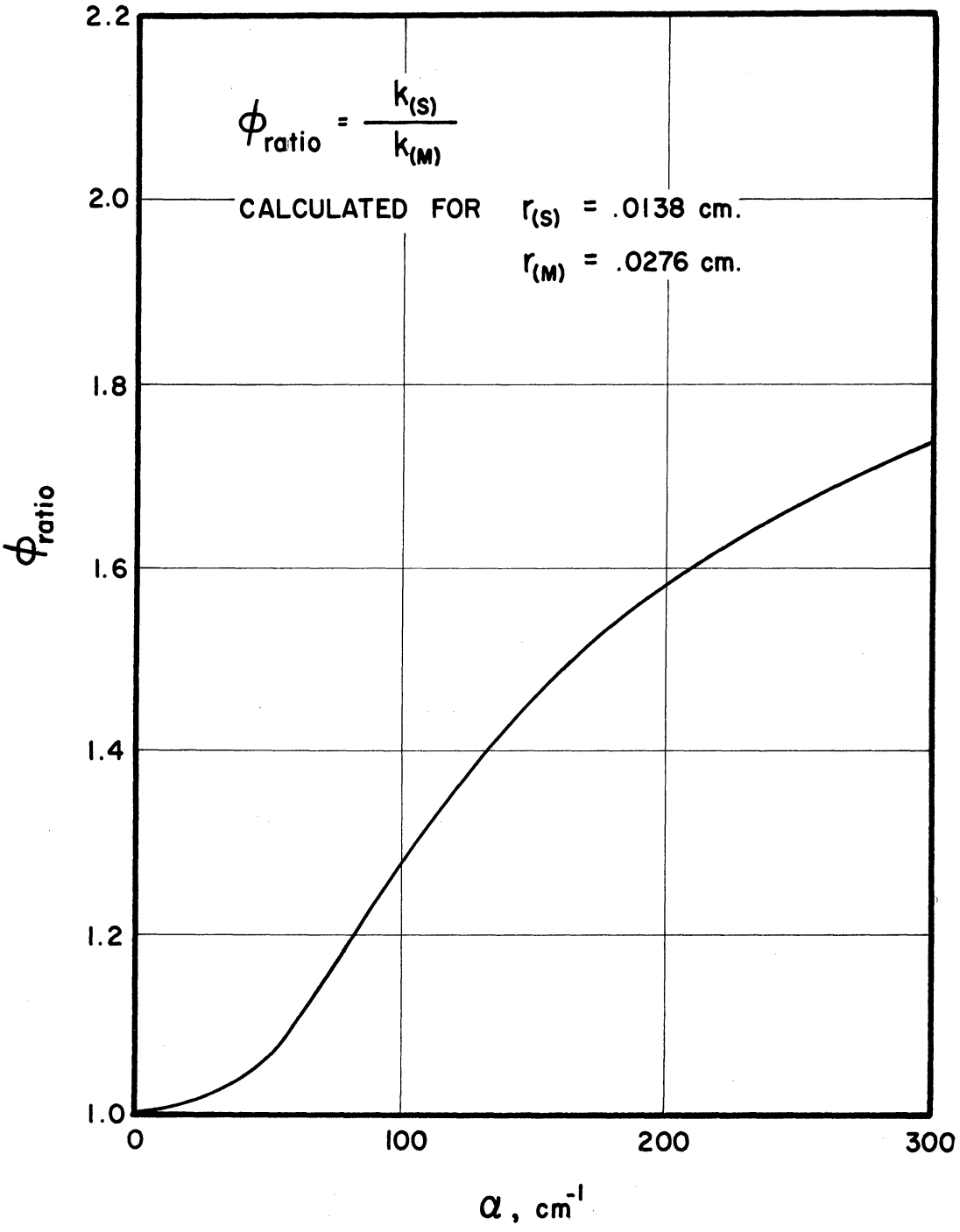

Figure 12. ϕ ratio versus α.

The effect of particle size was measured at three temperatures and three water concentrations; each T-C_w pair determined an experimental value of ϕ ratio, which was calculated from the ratio of k values and is listed in Table V. The corresponding value of α was determined from Figure 12 and it is also given in Table V.

A distinction is usually made between chemical- and diffusion-controlled rates, the former being those examples in which particle size appears to have no effect on the rate. This is never exactly true, since the diffusion process must result in an average particle concentration lower than the surface concentration, but as can be seen from Figure 12, for α less than 50 $cm.^{-1}$ the rates are not more than 5% different for the two particle sizes, i.e., they appear equal within experimental error. From Table V it can be seen that α averages about 150 $cm.^{-1}$ for the CHP decomposition reaction, so that more effective use is made of the catalyst if the particle size is small.

α is a function k_1 and D, both of which are expected to be similar functions of temperature. Since chemical rates usually have higher activation energies than diffusion rates, k_1 would be expected to increase more rapidly than D as the temperature is increased, and thus α would be a function of temperature. The values of α are plotted versus temperature with C_w as parameter in Figure 13; no significant trend is apparent. Likewise, Figure 14 shows that α is not a function of C_w. The interpretation is not made that α is actually independent of temperature. The factor λ also is expected to vary with temperature. The range of variables studied was apparently such that the two effects compensated each other. A satisfactory

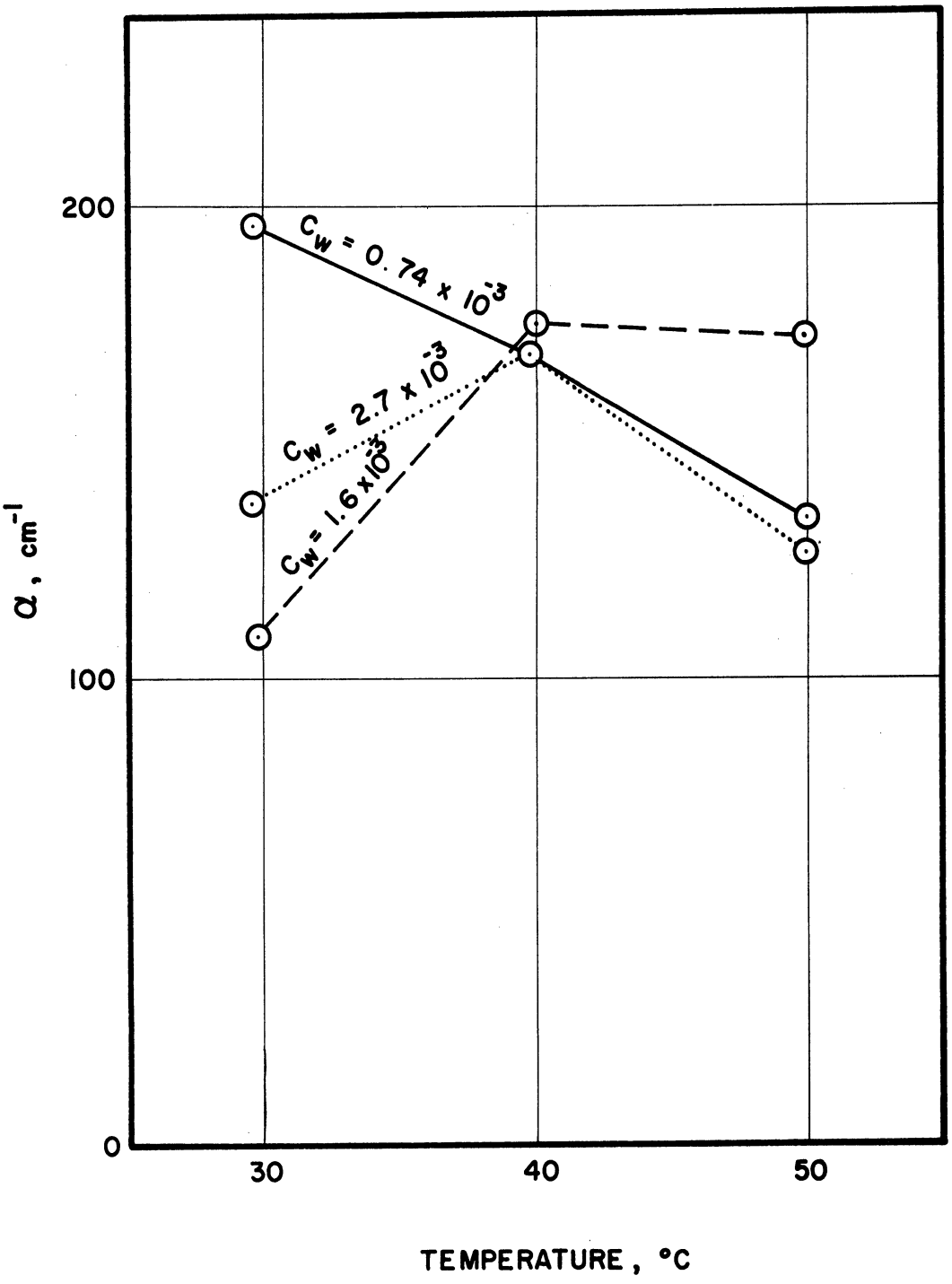

Figure 13. Effect of Temperature on α.

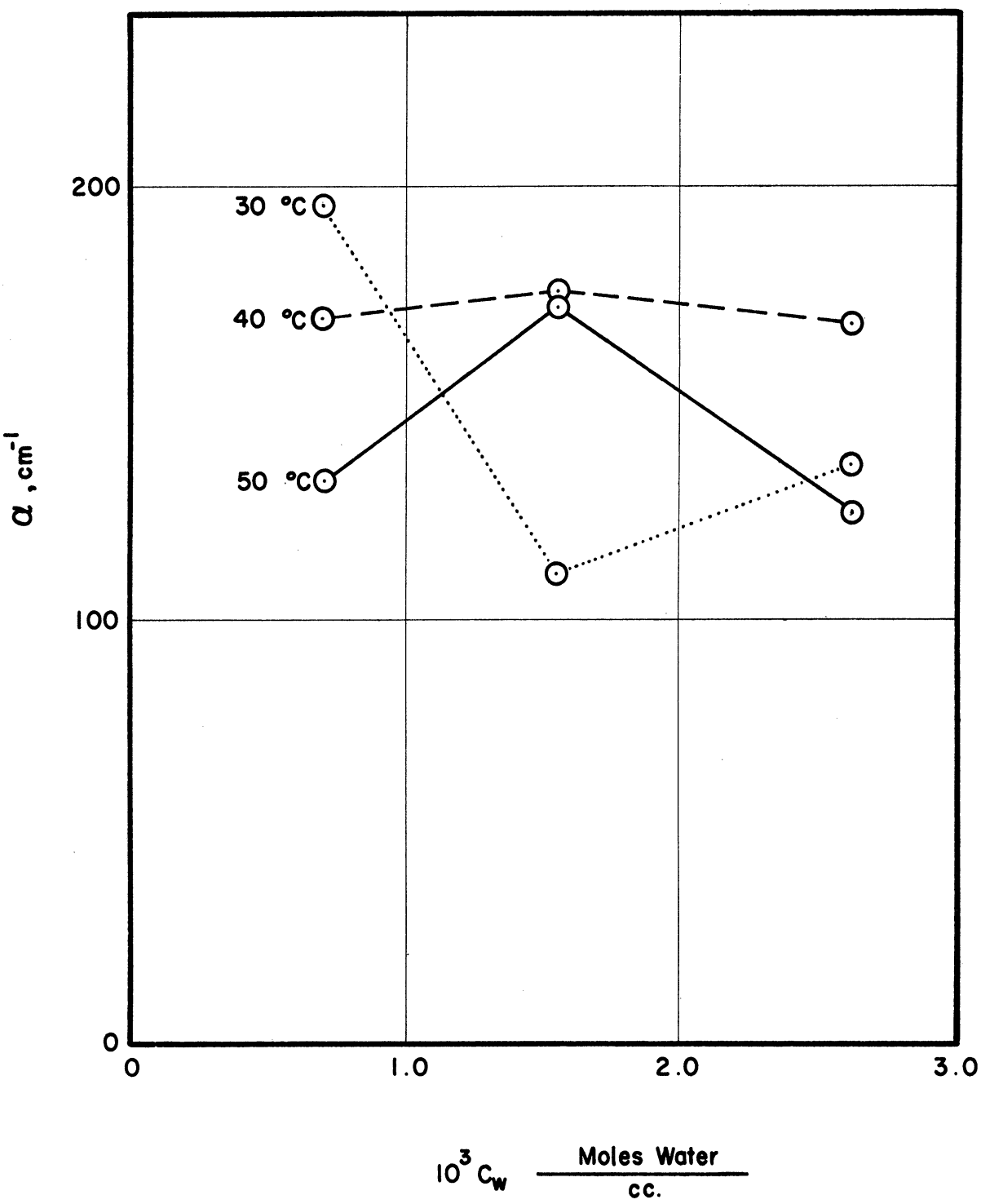

Figure 14. Effect of Water Content on α.

correlation is obtained by using a single average value of $\alpha = 150$ cm.$^{-1}$, making ϕ a function of radius only, and correlating temperature effects by $k_1 = f(T)$. The effect of particle size was thus correlated by

$$\phi = 1.33 \times 10^{-4} \left(\frac{150r \cosh 150r - \sinh 150r}{r^2 \sinh 150r}\right)$$

where r is the particle radius, cm.

The effect of changes in particle radius on the reaction rate due to changing environment (swelling of a given particle) can be estimated from the ϕ function and the ϕ ratio. With $\alpha = 150$ cm.$^{-1}$, $r_{(S)} = 0.0138$ cm., and $r_{(M)} = 0.0276$ cm., the ϕ ratio is calculated to be 1.45. The variation in $r_{(S)}$ was estimated at $\pm 2\frac{1}{2}\%$ from observations on the total bed volume in the glass reactor. For $\alpha = 150$ cm.$^{-1}$ and $r_{(S)} = 0.01415$ cm. (estimated maximum expansion), the ϕ ratio is calculated to be 1.46, from which a value of $\alpha = 155$ cm.$^{-1}$ is estimated; the variation in α due to resin swelling therefore is estimated to be much less than the observed experimental variation. The value of ϕ itself is calculated (for $\alpha = 150$ cm.$^{-1}$) as 0.798 for $r_{(S)} = 0.01415$ cm., which is less than 1% change. Thus the overall significance of errors resulting from not considering changes in particle radius over the range of conditions studied is slight.

The effect of temperature was correlated by variations in k_1:

$$k_1 = A \exp(-E/RT)$$

where A, E, and R are constants and T is in degrees Kelvin. With the equation defining k this gives

$$k = k_1(\rho/m)\phi\lambda = A(\rho/m)\phi\lambda \exp(-E/RT) = A'\phi\lambda \exp(-E/RT)$$

where $A' = A\rho/m$, a constant, and

$$\ln k = \ln A'\phi\lambda - E/RT$$

On a plot of ln k versus $1/T°K$, a family of straight parallel lines is predicted, each line being determined by the intercept $\ln A'\phi\lambda$, which is a function of r and the C_j. For a given composition, the k values from the small and medium particles give a pair of lines with the ratio of the coefficient $A'\phi\lambda$ equal to the ϕ ratio:

$$\frac{A'\lambda\ \phi(S)}{A'\lambda\ \phi(M)} = \frac{\phi(S)}{\phi(M)}$$

The experimental values of k from Table V are plotted as ln k versus $1/T°K$ in Figure 15. The value of ϕ ratio = 1.45, corresponding to the value of α = 150 $cm.^{-1}$, is used to determine the relationship between the pair of lines corresponding to the two particle sizes and a given composition. Variation in α is reflected by variation in the spacing between the pair of lines. For the pair corresponding to $C_W = 1.6 \times 10^{-3}$, for example, if α = 200 $cm.^{-1}$ had been used rather than α = 150 $cm.^{-1}$, the line correlating the temperature effect for the small particles (dotted line) would be shifted from a value of ln k of 2.79 to 2.90 at $1/T = 0.00320$, referred to a constant position for the line for the medium particles.

It has been assumed that only k_1 is a function of temperature, since no significant variation of α with temperature was found. Deviations from parallel straight lines will result if α is actually a function of temperature or if λ is. If α increases with temperature, the data for a given line will be convex upwards on a plot of ln k versus $1/T$.

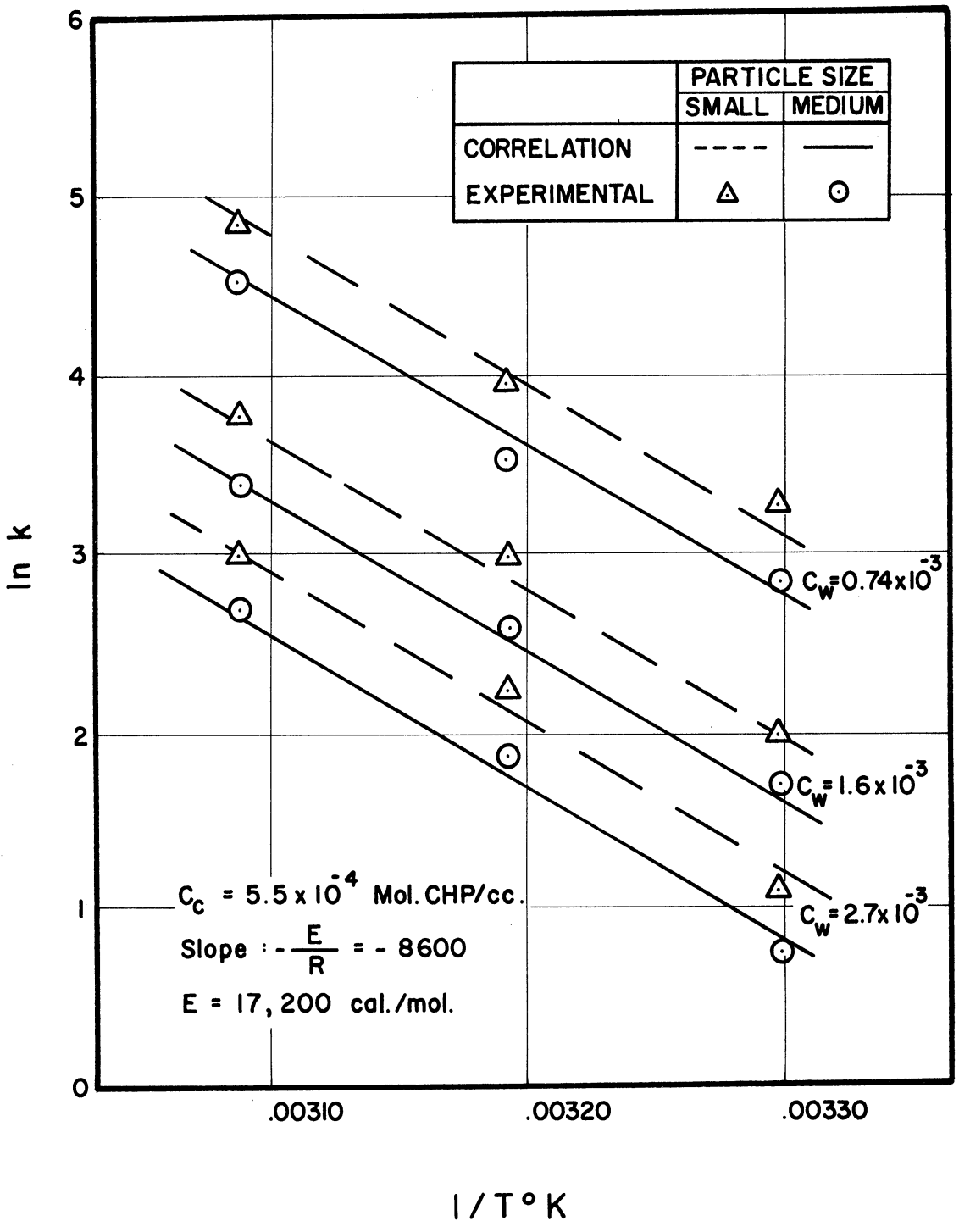

Figure 15. Correlation of Temperature.

The variation of λ with temperature is very likely. The effect of temperature was usually measured for a given feed composition by changing the temperature without stopping the feed after the first steady state was reached. The total volume of the bed usually changed when this was done, indicating that the volume of absorbed liquid changed. This was probably accompanied by a shift in the water-acetone ratio and therefore by a change in the CHP phase-distribution coefficient.

The slope of the lines in Figure 15 gives an activation energy of 17,200 calories; Tobolsky and Mesrobian[37] report an activation energy of 21,300 calories for the homogeneous reaction.

The intercept at $1/T = 0$ of the lines in Figure 15 is $\ln A'\phi\lambda$. The intercepts for the lines pertaining to the medium particles at each value of C_w are

C_w $\frac{\text{mol. water}}{\text{cc.}}$	$\ln A'\phi_{(M)}\lambda$	$A'\phi_{(M)}\lambda$
0.0027	29.22	4.90×10^{12}
0.0016	29.96	10.30×10^{12}
0.00074	31.12	32.9×10^{12}

Since $A'\phi_{(M)}$ is constant, the variation of $A'\phi_{(M)}\lambda$ with C_w reflects the variation of λ with C_w. No theoretical form for this relationship is known; it is approximately an inverse relationship. A two constant fit of the form

$$A'\phi_{(M)}\lambda = c_1(C_w)^{c_2}$$

is made by plotting $\ln A'\phi_{(M)}\lambda$ versus $\ln C_w$ (Figure 16), from which the constants are determined to be $c_1 = 7.10 \times 10^8$ and $c_2 = -1.49$.

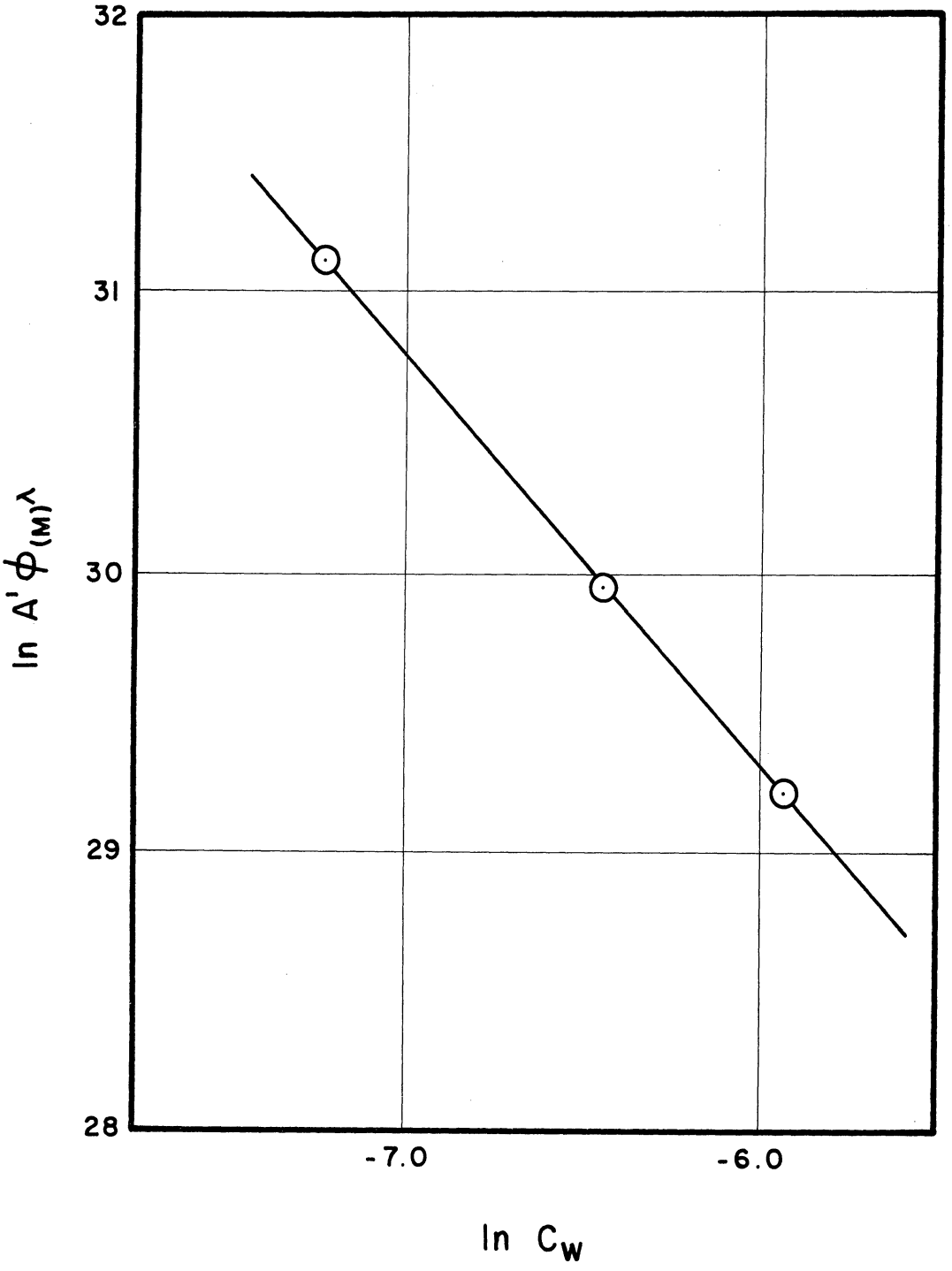

Figure 16. Correlation of Effect of Water Concentration on λ .

The data of Table V, which have been the basis for correlation to this point, were determined at $C_c = 5.5 \times 10^{-4}$ mol. CHP/cc. (10% CHP). Figure 10, page 59, gives the effect of increasing C_c. The data for the higher CHP concentrations can be correlated with the 10% CHP curve by replotting the data in terms of an effective C_w, where

$$C_{w(effective)} = C_w + 0.91\ (C_c - 0.00055)$$

This results in a single curve for the data (Figure 17). Since $C_{w(effective)} = C_w$ at $C_c = 5.5 \times 10^{-4}$, this relationship can be substituted into the correlation for λ, it having been derived at $C_c = 5.5 \times 10^{-4}$; thus

$$A'\phi_{(M)}\lambda = 7.10 \times 10^{8}[C_w + 0.91(C_c - .00055)]^{-1.49}$$

or, since $\phi_{(M)} = 0.550$

$$A'\lambda = 1.290 \times 10^{9}[C_w + 0.91(C_c - 00055)]^{-1.49}$$

The factor ρ/m has been considered constant in deriving the mathematical model and for purposes of correlation. It is actually a function of composition. ρ varies from 0.83 gm/cc. (10% CHP) to 0.88 gm./cc. (30% CHP). m varies as the quantity of liquid absorbed by the resin changes, and it is estimated as $\pm 2\frac{1}{2}\%$ change from observation of volume changes. The assumption of constant ρ/m in the model derivation applied only to the range of conditions in a bed at steady state. For a low conversion run, this range is small, and the assumption is a good approximation. In the correlation, the effect of composition change has been correlated by $A'\lambda = A\ \rho\lambda/m = f(C_j)$. The effect of changes in ρ/m

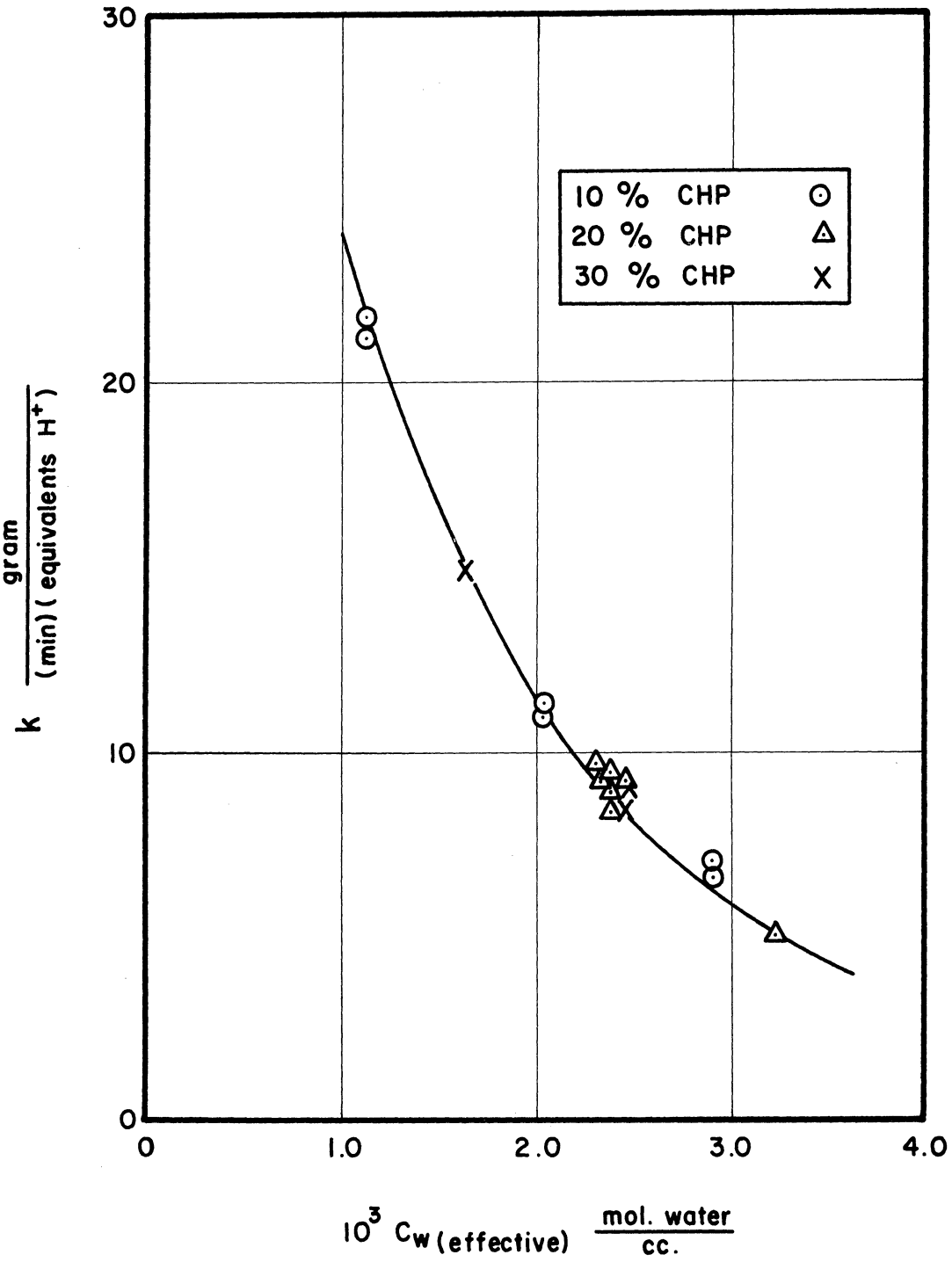

$$C_{w(\text{effective})} = C_w + 0.91\ (C_c - 5.5 \times 10^{-4})$$

Figure 17. Correlation of the Effect of C_c on k in terms of an Effective Water Concentration.

is thus included in the empirical correlation for composition effects. The single value of $m/\rho = 0.00435$ equiv. H^+/gram, estimated from volume and capacity measurements, is used in the rate correlation.

The final form of the rate correlation is obtained by combining the separate correlation for k_1, f, C_w, and C_c:

$$R = k(m/\rho)C_c = A\, e^{-E/RT}(m/\rho)(\rho/m)\phi\lambda C_c$$

$$= A'\lambda\phi\, C_c\, e^{-E/RT}(m/\rho)$$

$$= 1.29 \times 10^{9}[C_w + 0.91\,(C_c - .00055)]^{-1.49} \times$$

$$1.33 \times 10^{-4}\left(\frac{150r \cosh 150r - \sinh 150r}{r^2 \sinh 150r}\right) \times$$

$$.00435\, C_c \exp(-8600/T)$$

$$R = 7.46 \times 10^{+2}[C_w + 0.91\,(C_c - .00055)]^{-1.49} \times$$

$$\left(\frac{150r \cosh 150r - \sinh 150r}{r^2 \sinh 150r}\right) C_c \exp(-8600/T)$$

where R is the rate of decomposition, moles CHP per (min.)(cc.); C_w is the concentration of water, moles water/cc.; C_c is the concentration of CHP, moles CHP/cc.; r is the radius of Dowex 50 X 8 resin, cm.; and T is the temperature, °K.

Comparison of the correlation with the experimental data is made in Figures 18, 19, and 20 for $C_w = 0.74 \times 10^{-3}$, 1.6×10^{-3}, and 2.7×10^{-3} moles water/cc., respectively. The model gives good correlation while

maintaining a simple form. Because the effect of each variable was correlated by a separate factor, the model could not handle the interactions which observation indicated were presented, particularly that between temperature and the phase distribution coefficients. This deviation is considered the major cause of the differences between the correlation and the experimental data.

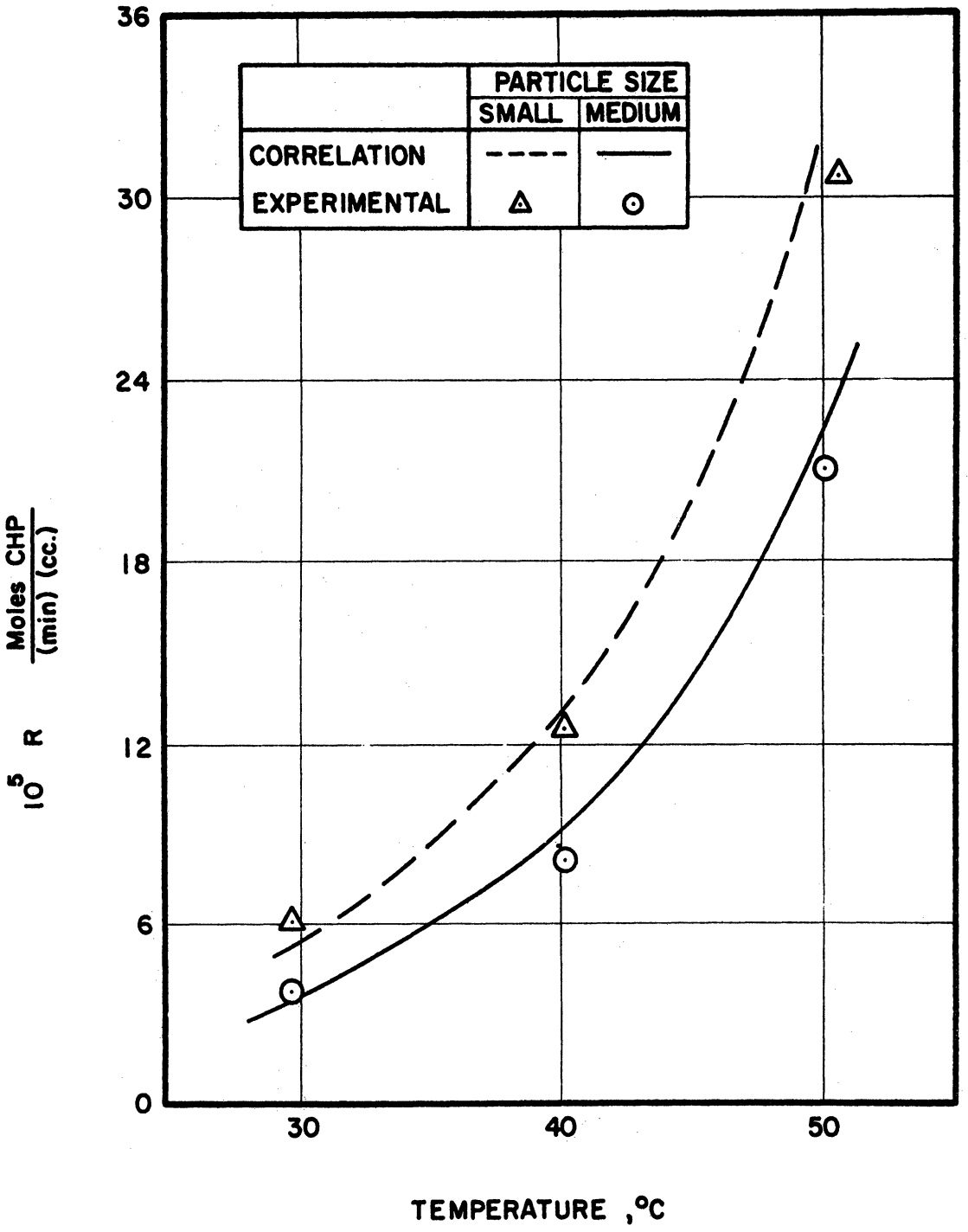

Figure 18. Comparison of Correlation with Experimental Data for $C_w = 0.74 \times 10^{-3}, C_c = 5.5 \times 10^{-4}$

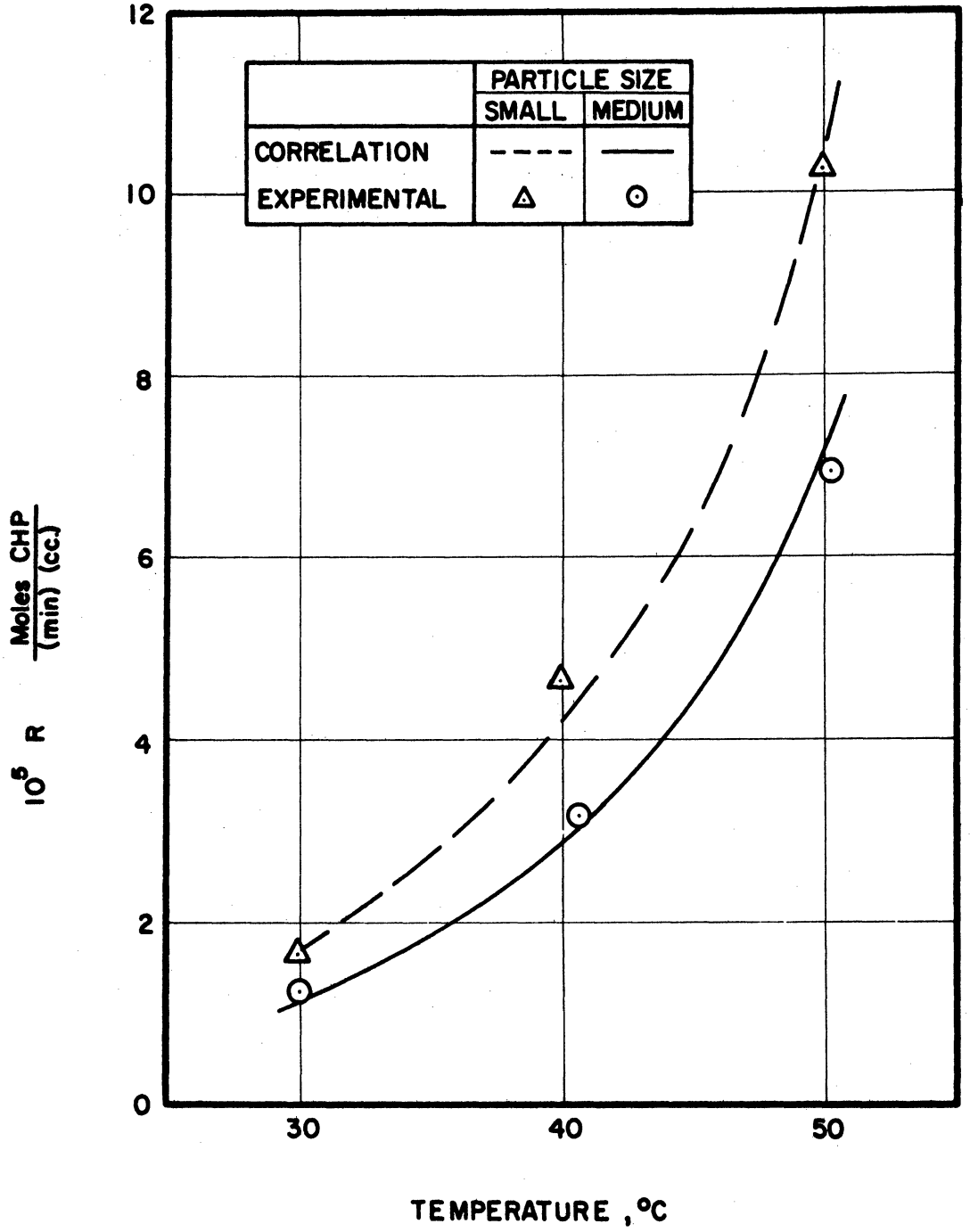

Figure 19. Comparison of Correlation with Experimental Data for $C_w = 1.6 \times 10^{-3}$, $C_c = 5.5 \times 10^{-4}$

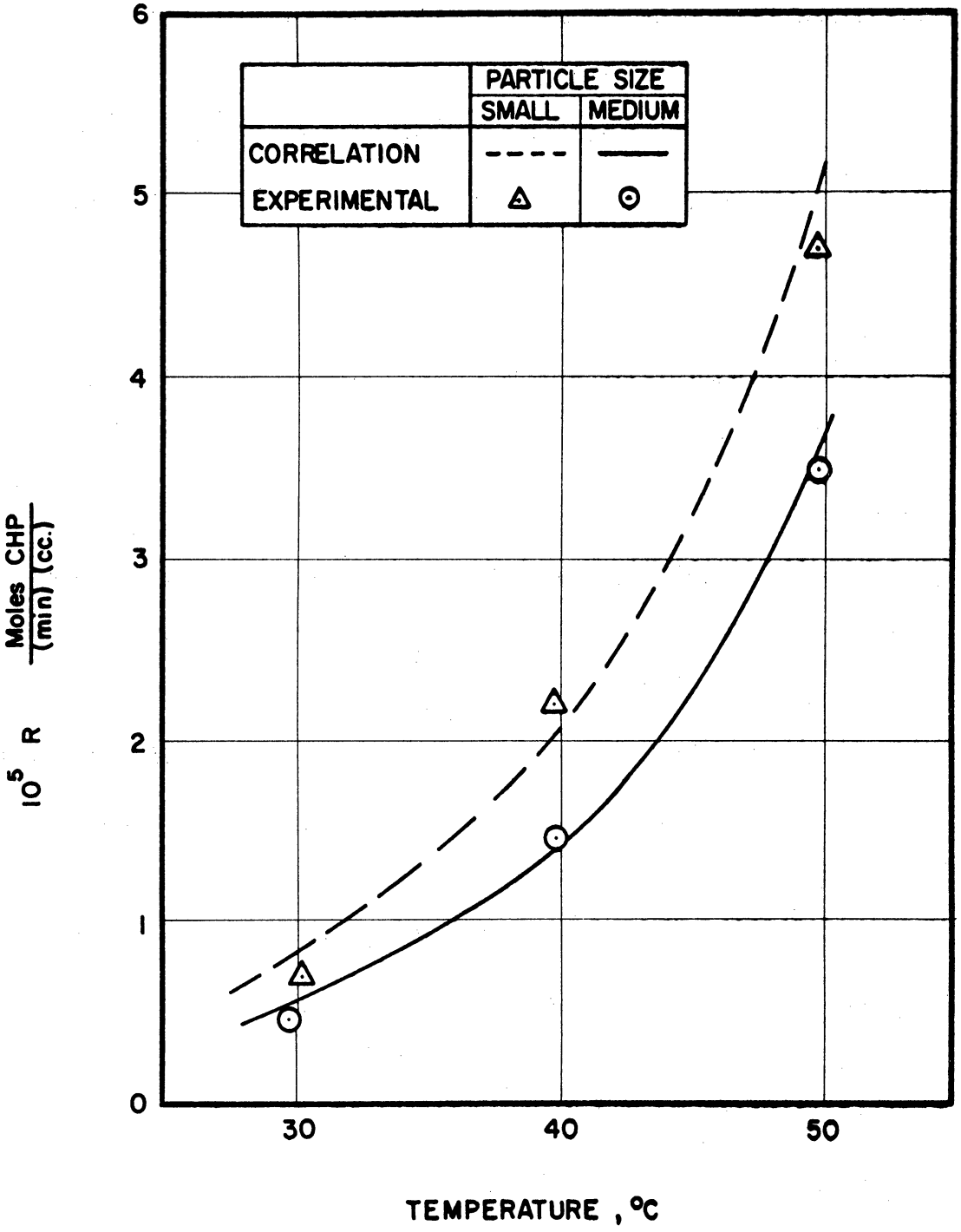

Figure 20. Comparison of Correlation with Experimental Data for $C_w = 2.7 \times 10^{-3}, C_c = 5.5 \times 10^{-4}$

CONCLUSIONS

(1) Dowex 50, a cross-linked sulfonated polystyrene resin, is a suitable catalyst when in acid form for promoting the decomposition of cumene hydroperoxide to phenol.

(2) The water concentration of the feed is an important factor in determining the rate of reaction, the rate in acetone varying inversely with the water concentration to the 3/2 power.

(3) The level of water concentration affects the behavior of the catalyst. Above 1.5% water, for 10% CHP and 50°C, the catalyst remains light in color, but below this value it darkens steadily until becoming black. The interpretation was made that the specificity of the reaction was high above 1.5% water but that secondary reactions become important below this value, the byproducts from these reactions causing the darkening.

(4) The particle size of the catalyst is a factor in determining the rate of this reaction. The smaller size gives the higher rate.

(5) The stability of the catalyst is good in the region of high water concentration. The maximum period of testing for a single catalyst batch was 165 hours. Under conditions which produce darkening the catalyst is more susceptible to breaking and "freezing" into place.

(6) The order of the reaction cannot be measured with this catalyst unless the interpretation is made that the order is a function of the water concentration. The concept of phase distribution coefficients which are functions of temperature and composition was introduced and used to interpret the experimental results in conjunction with an assumed order of reaction.

(7) The data were correlated by the following equation:

$$R = 7.46 \times 10^{2}[C_w + 0.91\ (C_c - .00055)]^{-1.49} \times$$

$$\left(\frac{150r \cosh 150r - \sinh 150r}{r^2 \sinh 150r}\right) C_c \exp(-8600/T)$$

R is the rate of decomposition, moles CHP per (min.)(cc.); C_w is the concentration of water, moles water/cc.; C_c is the concentration of CHP, moles CHP/cc.; r is the radius of the Dowex 50 X 8 resin particle, cm.; and T is the temperature, °K.

Several limitations should be observed in applying the equation. The data for the correlation were obtained only from Dowex 50 X 8 resin. The equation probably is not valid below $C_w = 0.7 \times 10^{-3}$ moles/cc. (1 1/2 wt. % water) due to increased secondary reactions. Above a feed flow rate of 4.0 grams per (min.)($cm.^2$) no effect of flow rate was observed. With these limitations the equation applies well over the ranges of variables studied. It predicts the experimental values with an average percent error of 7.3%.

APPENDIX A

TABULATION OF EXPERIMENTAL DATA

APPENDIX A

TABULATION OF EXPERIMENTAL DATA

Table A-1 Flow Effect

Run	$10^4 C_{ci}$	$10^4 C_{cf}$	W	N	Resin Type	$\ln \frac{C_{ci}}{C_{cf}}$	k	$10^3 C_w$	T
	$\frac{\text{moles CHP}}{\text{cm.}^3}$		$\frac{\text{gm.}}{\text{min.}}$	equiv.H^+ in reactor			$\frac{\text{gm.}}{\text{min.equiv.}}$	$\frac{\text{mol.water}}{\text{cm.}^3}$	°C
	initial	final	Flow rate						
12A	11.78	10.56	1.21	.0300	50X8(L)	.109	9.20	3.0	50.2
12B	11.78	9.32	2.53	.0300	50X8(L)	.233	9.40	3.0	49.8
12C	11.78	10.85	3.37	.0300	50X8(L)	.081	9.10	3.0	50.2
12D	11.80	11.28	5.84	.0300	50X8(L)	.045	8.76	3.0	50.2
30A	5.81	4.87	4.66	.00626	50X8(S)	.176	131.1	0.92	51.2
30B	5.81	5.02	3.12	.00376	50X8(S)	.146	121.1	0.92	50.5
30C	5.81	4.88	2.06	.00282	50X8(S)	.174	126.9	0.92	50.5
30D	5.81	4.94	1.52	.00189	50X8(S)	.162	130.2	0.92	50.5
15A	5.61	5.11	2.31	.0300	50X8(L)	.094	7.25	3.9	50.8
15B	5.61	4.35	0.84	.0300	50X8(L)	.255	7.15	3.9	49.3
17A	5.59	4.40	2.72	.0300	50X8(L)	.239	21.7	2.1	50.3
17B	5.59	3.89	1.76	.0300	50X8(L)	.363	21.3	2.1	50.3

Table A-2 Effect of Water

Run	$10^4 C_{ci}$	$10^4 C_{cf}$	W	N	Resin Type	$\ln \frac{C_{ci}}{C_{cf}}$	k	$10^3 C_w$	T
	$\frac{\text{moles CHP}}{\text{cm.}^3}$		$\frac{\text{gm.}}{\text{min.}}$	equiv.H^+ in			$\frac{\text{gm.}}{\text{min.equiv.}}$	$\frac{\text{mol.water}}{\text{cm.}^3}$	°C
	initial	final	Flow rate	reactor					
11	11.85	10.55	2.46	.0300	50X8(L)	.116	9.52	3.0	49.6
14	11.98	8.38	0.83	.0300	50X8(L)	.385	10.65	2.9	49.6
16	11.70	9.66	0.82	.0300	50X8(L)	.192	5.25	3.9	50.
18A	17.39	15.88	2.97	.0300	50X8(L)	.091	9.00	2.7	50.8
18B	17.39	12.99	0.94	.0300	50X8(L)	.033	10.35	2.7	50.4
19A	18.30	15.18	3.48	.0300	50X8(L)	.187	21.7	1.8	54.4
19B	18.30	12.45	1.80	.0300	50X8(L)	.385	23.1	1.8	54.3
21A	5.52	4.36	4.85	.0300	50X8(L)	.236	38.2	1.4	52.3
21B	5.52	5.11	2.50	.0300	50X8(L)	.077	6.41	1.4	29.5
22A	5.52	3.35	4.86	.0300	50X8(L)	.499	80.9	0.97	54.
22B	5.52	2.19	4.86	.0300	50X8(L)	.924	149.6	0.97	60.
23	5.71	4.59	4.79	.0300	50X8(L)	.218	34.8	0.46	31.0
25	5.82	2.01	1.90	.0300	50X8(L)	1.064	67.5	0.18	28.

Also Runs 12, 13, 15, 17, and 24. (See other tables.)

Table A-3 Particle Size Effect

Run	$10^4 C_{ci}$	$10^4 C_{cf}$	W	N	Resin Type	$\ln \frac{C_{ci}}{C_{cf}}$	k	$10^3 C_w$	T
	$\frac{\text{moles CHP}}{\text{cm.}^3}$		$\frac{\text{gm.}}{\text{min.}}$	$\frac{\text{equiv.H}^+}{\text{in}}$			$\frac{\text{gm.}}{\text{min.equiv.}}$	$\frac{\text{mol.water}}{\text{cm.}^3}$	°C
	initial	final	Flow rate	reactor					
32	6.00	5.42	2.15	.0712	50X8(S)	.101	3.05	2.7	30.5
33	6.00	5.01	3.65	.0712	50X8(S)	.180	9.24	2.7	40.
34	6.00	4.97	4.50	.0426	50X8(S)	.186	19.65	2.7	50.1
35	5.93	4.92	4.43	.0426	50X8(S)	.187	19.42	1.6	40.0
36	5.93	5.16	2.18	.0426	50X8(S)	.139	7.11	1.6	30.1
37	5.93	5.05	3.63	.0136	50X8(S)	.161	43.0	1.6	50.0
38	5.84	4.96	2.15	.0136	50X8(S)	.163	25.8	0.74	30.0
39	5.84	5.12	2.08	.00524	50X8(S)	.132	52.4	0.74	40.5
40	5.84	4.81	3.49	.00524	50X8(S)	.195	129.9	0.74	50.5
41	6.00	5.17	4.98	.0500	50X8(M)	.146	14.54	2.7	50.2
42	6.00	5.72	2.15	.0500	50X8(M)	.047	2.02	2.7	29.8
43	6.00	5.20	2.15	.0500	50X8(M)	.143	6.15	2.7	40.0
44	5.93	5.10	4.45	.0500	50X8(M)	.150	13.35	1.6	40.6
45	5.93	5.23	2.16	.0500	50X8(M)	.126	5.45	1.6	30.1
46	5.93	5.11	2.93	.0150	50X8(M)	.148	28.9	1.6	50.2
47	5.84	5.23	2.17	.0150	50X8(M)	.110	15.9	0.74	29.7
48	5.84	5.31	2.17	.0060	50X8(M)	.095	34.4	0.74	40.3
49	5.84	5.06	3.74	.0060	50X8(M)	.143	89.2	0.74	50.0
50	6.00	4.73	3.65	.0666	50X8(L)	.237	13.0	2.7	50.2
51	6.00	5.65	2.15	.0666	50X8(L)	.060	1.94	2.7	29.9
52	6.00	5.06	2.15	.0666	50X8(L)	.170	5.49	2.7	40.2
53	5.93	4.77	3.63	.0666	50X8(L)	.217	11.82	1.6	40.0
54	5.93	5.07	2.18	.0666	50X8(L)	.156	5.11	1.6	28.8
55	5.93	4.66	2.83	.0250	50X8(L)	.241	27.3	1.6	49.5

Table A-4 Other Effects: Reproducibility (13-60); Effect of Cross-linking (62-63); Resin Grade (64-65); and Cumene as Solvent (154-157)

Run	$10^4 C_{ci}$	$10^4 C_{cf}$	W	N	Resin Type	$\ln \frac{C_{ci}}{C_{cf}}$	k	$10^3 C_w$	T
	$\frac{\text{moles CHP}}{\text{cm.}^3}$		$\frac{\text{gm.}}{\text{min.}}$	$\frac{\text{equiv.H}^+}{\text{in}}$			$\frac{\text{gm.}}{\text{min.equiv.}}$	$\frac{\text{mol.water}}{\text{cm.}^3}$	°C
	initial	final	Flow rate	reactor					
13	5.70	4.68	1.72	.0300	50X8(L)	.197	11.3	3.0	49.7
24	5.91	4.98	1.95	.0300	50X8(L)	.172	11.2	3.0	50.5
39	5.84	5.12	2.08	.00524	50X8(S)	.132	52.5	0.74	40.5
59	5.84	5.21	2.09	.00465	50X8(S)	.114	51.2	0.74	40.5
40	5.84	4.81	3.49	.00524	50X8(S)	.195	130.0	0.74	50.5
60	5.84	4.89	3.34	.00465	50X8(S)	.177	127.1	0.74	50.5
62	5.95	4.87	2.16	.0484	50X4(M)	.201	8.97	2.7	39.8
63	5.95	4.42	4.17	.0484	50X4(M)	.297	25.6	2.7	49.5
64	5.96	5.44	3.74	.0599	50WX8(L)	.091	6.09	2.7	39.8
65	5.95	5.56	2.15	.0599	50WX8(L)	.070	2.69	2.7	49.5
154	12.28	11.76	0.86	.0066	50X8(S)	.043	5.60	0.29	50.0
155	12.32	11.67	0.96	.0066	50X8(S)	.054	7.86	0.35	50.0
156	12.36	11.42	0.96	.0066	50X8(S)	.079	11.50	0.42	50.0
157	12.20	10.99	0.96	.0066	50X8(S)	.104	15.12	0.48	50.0

APPENDIX B

ESTIMATION OF PARTICLE TEMPERATURE

APPENDIX B

ESTIMATION OF PARTICLE TEMPERATURE

The equation for temperature as a function of particle radius is derived from an energy balance on the spherical element referred to in Figure 2, page 19:

in (diffusion) - out (diffusion) + in (mass transfer)

- out (mass transfer) = 0.

Since all the CHP transferred into a sphere of radius x reacts to proportionate quantities of phenol and acetone (100% yield assumed) which are then transferred out of the sphere, at either surface of the element the total mass transfer may be expressed in terms of the CHP diffusion rate w mol per (min.) (cm.^{2}), and the energy transferred is expressed by the enthalpies H_j cal./mole of the components:

$$q A + (q + dq)(A + dA) + w A(H_p + H_a - H_c) - (w + dw)(A + dA)(H_p + H_a - H_c + dH_p + dH_a - dH_a) = 0 \quad (35)$$

q is the rate of heat transfer, cal. per (min.)(cm.^{2}), due to the temperature gradient. The enthalpy terms are combined to give the heat of reaction:

$$(H_p + H_a - H_c) = \Delta H \quad (36)$$

and the differentials combine to give $d\Delta H$:

$$(dH_p + dH_a - dH_c) = d\Delta H \quad (37)$$

Substituting Equations (36) and (37) into (35), expanding the terms, dividing by (dx) and neglecting the differential terms gives

$$-2qx - x^2\left(\frac{dq}{dx}\right) - w\Delta H 2x - w\left(\frac{d\Delta H}{dx}\right)x^2 - \Delta H\left(\frac{dw}{dx}\right)x^2 = 0 \quad (38)$$

The rate of heat transfer q is expressed by

$$q = -b\frac{dT}{dx} \tag{39}$$

and the differential flow rate dq/dx is expressed, assuming the thermal conductivity b is not a function of x, by

$$\frac{dq}{dx} = -b\frac{d^2T}{dx^2} \tag{40}$$

The expressions for w and dw/dx as functions of C', from page 20, are:

$$w = -D\frac{dC'}{dx} \qquad \frac{dw}{dx} = -D\frac{d^2C'}{dx^2}$$

The expressions for q, dq/dx, w, and dw/dx are substituted into Equation (38); a further assumption, that $d\Delta H/dx = 0$ because of a low temperature rise, is incorporated, and the result is, with rearranging:

$$x^2\frac{d^2T}{dx^2} + 2x\frac{dT}{dx} + \frac{\Delta H D}{b}\left[2\alpha\left(\frac{dC'}{dx}\right) + \alpha^2\left(\frac{d^2C'}{dx^2}\right)\right] = 0 \tag{41}$$

Equation (41) is combined with Equations (15) and (19), pages 22 -24, to give an equation in T and x only:

$$x^2\frac{d^2T}{dx^2} + 2x\frac{dT}{dx} + \frac{\Delta H k_1}{b}C_s' x^2\frac{\alpha r}{\alpha x}\frac{\sinh(\alpha x)}{\sinh(\alpha r)} = 0 \tag{42}$$

This may be solved with the boundary conditions

(1) $dT/dx = 0$ at $x = 0$

(2) $T = T_s$ at $x = r$

The equation is reduced to a linear first order equation by the substitution $dT/dx = z$ and solved for z; integration gives the final solution.[34]

$$T = T_s + \frac{\Delta H k_1 C_s'}{b\alpha^2}\left(\frac{\sinh(\alpha x)}{\sinh(\alpha r)}\cdot\frac{\alpha r}{\alpha x} - 1\right)$$

The maximum temperature rise $T - T_s$ that can occur within the particle is equal to the coefficient of the variable term, since

$$0 < \frac{\sinh(\alpha x)}{\sinh(\alpha r)} \cdot \frac{\alpha r}{\alpha x} \leqslant 1$$

A value of the coefficient is calculated from these estimates of the constants:

$$\Delta H = -60{,}600 \text{ cal./mol. CHP}$$

$$b = .025 \text{ cal. per (cm.)(min.)(°C)}$$

$$k_1/\alpha^2 = D = 10^{-4} - 10^{-7} \text{ cm.}^2/\text{min.}$$

$$C_s' = 1.7 \times 10^{-3} \text{ mol. CHP/cc. soln.}$$

Thus,

$$T - T_s = \frac{-\Delta H k_1 C_s'}{b\alpha^2} = \frac{60{,}600 \times 10^{-4} \times 1.7 \times 10^{-3} \times 0.38}{2.5 \times 10^{-2}} = 0.16\,^{\circ}C$$

The method of estimating ΔH has been explained previously; b was estimated from the thermal conductivity of benzene and acetone; the value of D cannot be estimated with much more significance than is indicated, in this environment, so the more critical value was used; and C_s' was estimated for $\lambda = 1.0$. The rise in temperature of only 0.16°C that results is quite small. For activation energies of 18,000 cal./mol. for (k_1) and 9,000 cal./mol. for D, the ratio will vary by less than 1% for a temperature change of this magnitude. The assumption of constant α as a basis for solving Equation (15), page 22, seems reasonable.

APPENDIX C

SAMPLE CALCULATIONS AND EXPERIMENTAL MEASUREMENTS

APPENDIX C

SAMPLE CALCULATIONS AND EXPERIMENTAL MEASUREMENTS

The data of run 38 (Table A-3, Appendix A) are used to illustrate the procedure of operation. This run was part of the series using the small size (115-150 mesh) resin, with acetone as the solvent. Nominal conditions of 30°C, 10% (wt.) CHP, and 2% (wt.) water were selected. A k value of about 25 grams per (min.)(equiv. H^+) was estimated from previous work as the probable result. From $W_{min.} = 2.00$ gm./min., $\ln (C_{ci}/C_{cf}) = 0.163$ at 15% conversion, $k = 25$, and $k = \frac{W}{N} \ln (C_{ci}/C_{cf})$, the quantity of resin desired was calculated as $N = 0.0130$ equiv. H^+. The capacity of the resin had been measured as 4.68 milliquivalents per gram. A sample of 2.9100 grams of 115-150 mesh Dowex 50 X 8 was charged to the reactor, giving

$$N = \frac{4.68 \times 2.91}{1000} = 0.0136 \text{ equiv. } H^+$$

For the low flow rate to be used, a period of 4-6 hours to determine the steady state values was anticipated. Sufficient feed was prepared to obtain the data for three particle sizes at three temperatures from the one batch of feed (nine runs). The quantities weighed out and the approximate composition resulting were

1176 gms. stock (70 wt. %) CHP	10% CHP
	4% cumene
115 gms. water	2% water
6709 gms. acetone	84% acetone

The following titrations were made to observe the approach to steady state:

time after start-up, hrs.	volume of sample, cc.	ml. sodium thiosulfate
2.25	0.95	9.31
	0.95	9.41
3.0	0.95	9.42
	0.95	9.42
4.0	0.95	9.43
	0.95	9.40

The steady state value of 9.42 ml. $Na_2S_2O_3$ for 0.95 cc. sample was used. The feed analysis was 9.35 ml. $Na_2S_2O_3$ for 0.80 cc. sample. Thus:

$$C_{ci} = \frac{9.35}{0.80 \times 2000} = 5.84 \times 10^{-4} \text{ mol. CHP/cc.}$$

$$C_{cf} = \frac{9.42}{0.95 \times 2000} = 4.96 \times 10^{-4} \text{ mol. CHP/cc.}$$

$$\ln \frac{C_{ci}}{C_{cf}} = \ln \frac{5.84 \times 10^{-4}}{4.96 \times 10^{-4}} = \ln 1.178 = 0.163$$

The volumetric flow rate was measured during the steady state period by removing 3.00 cc. from a filled 25 ml. volumetric flask with a syringe and measuring the time to refill the flask with the output from the reactor. The time was 1.15 minutes. The density was measured by weighing 1.00 cc. of feed in a closed bottle, the result being 0.824 grams/cc. Thus

$$W = \frac{3.00 \text{ cc.} \times 0.824 \text{ gm./cc.}}{1.15 \text{ min.}} = 2.15 \text{ gm./min.}$$

The value of k is calculated from these values:

$$k = \frac{W}{N} \ln \frac{C_{ci}}{C_{cf}} = \frac{2.15 \times 0.163}{0.136} = 25.8 \frac{\text{gram}}{(\text{min.})(\text{equiv. } H^+)}$$

The axial thermocouple (copper-constantin), located at the mid-point of the bed, gave 1.20 m.v. in reference to a cold junction at 0°C. This corresponded to a temperature of 30.0°C. The thermocouple readings observed during calibration agreed within 0.01 m.v. of the standard values for copper-constantin thermocouples, which is a variation of 0.25°C in this range of operation.

The water concentration of the feed was measured as follows:

	Sample	ml. reagent
A.	25 cc. solvent	46.3
B.	25 cc. solvent + 0.0982 gm. water	69.6
C.	25 cc. solvent + 2.00 cc. feed	52.5

The titer of the reagent: $\frac{0.0982 \times 1000}{69.6 - 46.3} = \frac{4.21 \text{ mg. water}}{\text{ml. reagent}}$; ml. reagent for sample only: $52.5 - 46.3 = 6.2$.

Thus:

$$C_w = \frac{6.2 \text{ ml.}}{2.00 \text{ cc.}} \times 4.21 \frac{\text{mg.}}{\text{ml.}} \times \frac{1 \text{ mole water}}{18{,}000 \text{ mg.}} = 0.74 \times 10^{-3} \frac{\text{mol.}}{\text{cc.}}$$

The method of correlating the data is summarized as follows. The value of the φ ratio at given levels of water concentration and temperature was calculated from the ratio of the k values obtained with the small and medium size resin particles (Table V, page 73) and the corresponding value of α was determined from Figure 12, page 74. No effect of temperature on α was indicated (Figure 13), so an average value of 150 cm.$^{-1}$ was used in the φ function, which was assumed independent of temperature. This correlated the effect of particle size. The data of Table V were then plotted as an inverse temperature function (Figure 15, page 80). By trial and error, the slope for the family of parallel lines was determined graphically to give a minimum deviation of the group of data points from the family of lines. The spacing of the intercepts for the pair of lines at a given water concentration corresponding to the data from the samll and medium resin sizes was controlled as required by the assumption that α = 150 cm.$^{-1}$ A first trial for correlating the effect of water concentration on the phase distribution coefficient showed such a slight curvature on a log-log plot that the location of the central pair of lines in Figure 15 could be shifted sufficiently relative to the other two pairs to permit correlation of the composition effect by a two constant fit (Figure 16, page 82) without introducing large deviations from the experimental data. The correlation was completed by finding a simple function which expressed the interaction between the water and CHP concentrations.

The data from a number of runs were not included in the correlation nor listed in Appendix A. These were in the nature of exploratory runs and the level of water concentration was intermediate between those used for correlation.

BIBLIOGRAPHY

1. Tobolsky, A. V., and Mesrobian, R. B. Organic Peroxides. New York: Interscience Publishers, (1954), 107.

2. Leffler, J. E. J. Am. Chem. Soc., 72, (1950), 67.

3. Leffler, J. E. The Reactive Intermediates of Organic Chemistry. New York: Interscience Publishers, (1956), 168.

4. Fordham, J. W. L., and Williams, H. L. CADO Technical Index. ATI 84313, (1950).

5. Seubold, F. H., Jr. and Vaughan, W. E. J. Am. Chem. Soc., 75, (1953), 3790.

6. Kharasch, M. S., Fono, A., and Nudenberg, W. J. Org. Chem., 15, (1950), 748, 763.

7. Kharasch, M. S., Fono, A., and Nudenberg, W. J. Org. Chem., 16, (1951), 113.

8. Handbook of Chemistry and Physics, 40th Ed., Cleveland, Ohio: Chemical Rubber Publishing Co., (1959), 1898.

9. Fortuin, J. P., and Waterman, H. I. Chem. Eng. Sci., 2, (1953), 182.

10. Wenner, R. R. Thermochemical Calculations. New York: McGraw-Hill Book Company, (1941), 164.

11. Klotz, I. M. Chemical Thermodynamics. New York: Prentice-Hall, (1950), 172.

12. Topp, N. E., and Pepper, K. W. J. Chem. Soc., (1949), 3299.

13. Bauman, W. C., and Eichhorn, J. J. Am. Chem. Soc., 69, (1947), 2830.

14. Sundheim, B. R., Waxman, M. H., and Gregor, H. P. J. Phys. Chem., 57, (1953), 974.

15. Reichenberg, D., Pepper, K. W., and McCauley, D. J. J. Chem. Soc., (1951), 493.

16. Pepper, K. W., Reichenberg, D., and Hale, D. K. J. Chem. Soc., (1952), 3129.

17. Richardson, R. W. Nature, 164, (1949), 916.

18. Hale, D. L., Packham, D. I., and Pepper, K. W. J. Chem. Soc., (1953), 844.

19. Davies, C. W., and Thomas, G. G. J. Chem. Soc., (1951), 2624.

20. Govindan, K. P., and Bafna, S. L. Ind. Eng. Chem., 48, (1946), 310.

21. Govindan, K. P., and Bafna, S. L. J. Sci. Ind. Res., 16B, (1957), 321.

22. Reichenberg, D., and Wall, W. F. J. Chem. Soc., (1951), 493.

23. Davies, C. W., and Owen, B. D. R. J. Chem. Soc., (1956), 1676.

24. Boyd, G. E., Adamson, A. W., and Myers, L. S., Jr. J. Am. Chem Soc., 69, (1947), 2836.

25. Wilson, S., and Lapidus, L. Ind. Eng. Chem., 48, (1956), 994.

26. Smith, N. L., and Amundson, N. R. Ind. Eng. Chem., 43, (1951), 2156.

27. Bernhard, S. A., and Hammett, L. P. J. Am. Chem. Soc., 75, (1953), 5834.

28. Haskell, V. C., and Hammett, L. P. J. Am. Chem. Soc., 71, (1949), 1284.

29. Wadman, W. H. J. Chem. Soc., (1952), 3051.

30. Bernhard, S. A., and Hammett, L. P. J. Am. Chem. Soc., 75, (1953), 1798.

31. Helfferich, F. J. Am. Chem. Soc., 76, (1954), 5567.

32. Saletan, D. I. Ph.D. Thesis, University of Michigan (1950).

33. Barker, G. E. Ph.D. Thesis, University of Michigan (1952).

34. Mickley, H. S., Sherwood, T. K., and Reed, C. E. Applied Mathematics in Chemical Engineering. New York: McGraw-Hill Book Company, (1957), 141, 174.

35. Hercules Powder Company, Tech. Ser. Bull., No. 205, 1954.

36. Kokatnur, V. R., and Jelling, M. J. Am. Chem. Soc., 63, (1941), 1432.

37. Siggia, S. Quantitative Organic Analysis. New York: John Wiley and Sons, (1954), 100.

38. Lykken, L., Tresider, R. S., and Zahn, V. Ind. Eng. Chem., Anal. Ed., 18, (1946), 103.

39. Peters, E. D., and Jungnickel, J. L. Anal. Chem., 27, (1955), 450.

40. Mitchell, J., and Smith, D. M. Aquametry. New York: Interscience Publishers, (1948), 142.

41. Davies, C. W., and Thomas, G. G. J. Chem. Soc., (1952), 1607.

42. Klein, F. G. Ph.D. Thesis, University of Michigan (1955).

43. Reed, L. M., Wenzel, L. A., and O'Hara, J. B. Ind. Eng. Chem., 48, (1956), 205.